7-18-2017

Biomechanics of Snoring and Sleep Apnea

Charles F. Babbs
Purdue University, babbs@purdue.edu

Biomechanics of Snoring and Sleep Apnea

Charles F. Babbs, MD, PhD

Weldon School of Biomedical Engineering, Purdue University, West Lafayette, Indiana, United States of America

Abstract

To understand the mechanisms of snoring and sleep apnea a first-principles biomechanical analysis was done for airflow through branched parallel channels, separated by a freely movable soft palate, and converging to a common channel at the base of the tongue in a "Y-shaped" configuration. Branches of the Y describe slit-like passages on the nasal and oral sides of the soft palate, when the palate is pushed by backward movement of the tongue to form a wedge between the tongue surface and the posterior pharyngeal wall. The common channel of the Y describes the oropharyngeal passage between the base of the tongue and posterior pharyngeal wall. Channel resistances are characterized by a generalized Poiseuille Law for laminar flow. Pressure changes from flow through channel resistances and also from the Venturi effect are specified quantitatively. The resulting equations are solved both algebraically and numerically to describe motion of the soft palate and tongue during snoring and sleep apnea. Soft tissue motions are produced by counterbalanced Venturi pressures on opposite sides of the soft palate and by counterbalanced Venturi pressure and elastic recoil at the base of the tongue. Multiple physical mechanisms were discovered that can produce tissue motion at typical snoring frequencies in this system, some with the mouth open and some with the mouth closed. These palatal and tongue movements resemble motions of pendulums that oscillate in potential energy wells. Specific physical conditions leading to sleep apnea are identified, in which narrow gaps and unbalanced Venturi pressures lead to stable and effort-independent airway occlusion. The present analysis shows how the phenomena of both snoring and sleep apnea are fundamentally related and are governed by the same equations.

KEYWORDS: airway resistance, biomechanics, hypopnea, obstructive sleep apnea, pharynx, sleep disordered breathing, upper airway physiology

*Email: babbs@purdue.edu

Introduction

Many people do not sleep quietly. They snore. In addition to being annoying to sleep partners and family members, snoring can be medically significant. Factors that predispose to snoring, such as obesity, also increase the risk of sleep apnea [1]. In episodes of sleep apnea the upper airway is obstructed by posterior positioning of the base of the tongue so as to totally occlude the airway [2-4]. Unconsciously, the sleeper experiences respiratory distress, falling blood oxygen saturation, autonomic nervous system activation with raised blood pressure, and then partial arousal leading to a change in body position or muscle tone in the tongue that relives the airway obstruction temporarily until another apnea ensues. The resulting sleep fragmentation leads to a host of medical issues, including daytime sleepiness, automobile accidents, high blood pressure, pre-diabetes, chronic tiredness, de-conditioning, and weight gain [5].

The mechanical events underlying snores and sleep apnea are complex and variable. Direct endoscopic observations during sleep have revealed various modes of snoring in different individual sleepers, including audible and sub-audible frequency oscillations of the soft palate and uvula, pharyngeal walls, epiglottis, and tongue [6]. Beck and coworkers[7] recorded human sleeper's snores in the range of 60 to 300 Hz with a variety of simple to complex waveforms in the time domain. Liistro and coworkers [8] found lower time domain frequencies in the range of 25 to 75 Hz. The most commonly observed form of snoring involves vibration of the soft palate during inspiration [7, 9-11].

Computed tomographic (CT) studies show that snorers tend to have upper airway narrowing [12]. Snorers also have greater upper airway collapsibility (compliance) [13], which is associated with a sleep related decrease in tone of upper airway muscles [14, 15]. With less muscle tone during sleep, upper airway collapse and flow restriction may occur, resulting in sleep apnea. In heavy snorers more negative intrathoracic pressure is required during inspiration to overcome partial pharyngeal obstruction [16], and in severe cases of obstructive sleep apnea the tongue is drawn into stable contact with the posterior pharyngeal wall, completely blocking the airway [3]. Thus snoring can be considered as part of the spectrum of sleep disordered breathing, ranging from non-snoring, to benign snoring, to obstructive e sleep apnea [1].

Even today, more research is needed to understand the full range of anatomic, physiologic, and biomechanical factors that are involved in snoring and sleep apnea. Exactly how and why do tissues vibrate in settings with reduced space for airflow, especially in the supine position when the tongue falls backward, further narrowing the airway, or after use of alcohol or sedative drugs that further reduce muscle tone? Also, why under certain circumstances do the forces on upper airway soft tissues create effort-independent and biomechanically stable obstruction to airflow, that is, obstructive sleep apnea, with resultant daytime sleepiness, degraded quality of life and health, and the real threat of lethal automobile accidents?

At present there is no compact and satisfying explanation of why snoring occurs or how snoring can transform into sleep apnea. This paper describes a fresh, first-principles investigation of the underlying biophysics. The goals are to answer the following questions. Why does snoring happen? Why does sleep apnea happen? How are snoring and sleep apnea related? What

structures and what forces are involved? What variables govern the development, frequency, and loudness of snoring? What variables govern the onset of sleep apnea?

Methods

Structure of a biomechanical model

Figure 1 illustrates a three-channel, palatal shuttle mechanism. The model is based upon the relevant human anatomy, especially in the supine position, when snoring is most likely. During sleep, the tongue falls downward and posteriorly. In this position the palate forms a wedge between the base of the tongue and the posterior pharyngeal wall. This wedge creates three slit-like channels for airflow from the nose and mouth into the oropharynx, which come together in the shape of a "Y". The nasopalatal Channel 1 lies between the soft palate and the posterior pharyngeal wall. The oropalatal Channel 2 lies between the soft palate and the base of the tongue. These two functionally parallel channels merge to form the common oropharyngeal Channel 3. With the soft palate in the wedge position, these three channels collectively form a "narrows" with the potential to restrict airflow. Variables x_1, x_2, and x_3 represent the slit widths of Channels 1, 2, and 3 respectively. Variables x_1 and x_2 sum to a constant value; that is, as x_1 decreases, x_2 increases and vis versa. Variable x_3, representing the distal common channel of the "Y", is independent of variables x_1 and x_2. The initial values of these variables at time zero of the analysis or simulation represent equilibrium positions for any particular combination of gravity and muscle tone. In turn, and for simplicity, it is not necessary to include gravity explicitly in further detailed analysis.

Functionally the Y-shaped arrangement of channels forms small network of parallel and series resistances to airflow (Figure 1, inset). The sum of the flows in Channels 1 and 2 equals the flow in Channel 3. The resistance to airflow in narrow nasopalatal region of Channel 1, R_{p1}, is augmented by the series resistance to airflow through the nose, R_1, which is normally small compared to the narrows resistance. The resistance to airflow in the narrow oropalatal region of Channel 2, R_{p2},, is augmented by the series resistance to airflow through the mouth, R_2, which is small with the mouth open, intermediate with the mouth partially closed, and infinite with the mouth tightly closed. The augmented nasal and oral channel resistances can be expressed as

$$R'_1 = R_1 + R_{p1} \quad \text{and} \quad R'_2 = R_2 + R_{p2}. \tag{1}$$

Let R_3 be defined as the resistance to airflow through common Channel 3 and R_{aw} be defined as the normal airway resistance of the tracheobronchial tree, as is customary in respiratory physiology. Then in cases of partial upper respiratory tract obstruction associated with snoring and sleep apnea, the total airway resistance becomes

$$R_{tot} = \frac{R'_1 R'_2}{R'_1 + R'_2} + R_3 + R_{aw}\,. \tag{2}$$

This expression is the sum of the resistance of the parallel combination of Channels 1 and 2 (first term), in series with the resistance of Channel 3 and classical airway resistance. The resistances R_1, R_2, and R_3 depend upon a particular prevailing geometry in a particular body position. They are roughly approximated assuming a racetrack shaped cross section, as specified in Appendix 1. They can be adjusted as model constants at time zero for various desired configurations, such as mouth open vs. mouth closed, adult vs. child, large vs. small adenoids, etc. Since R_1, R_2, and R_3 are often relatively small, compared to R_{p1}, R_{p2}, and R_{aw} during active snoring, these rough estimates are satisfactory.

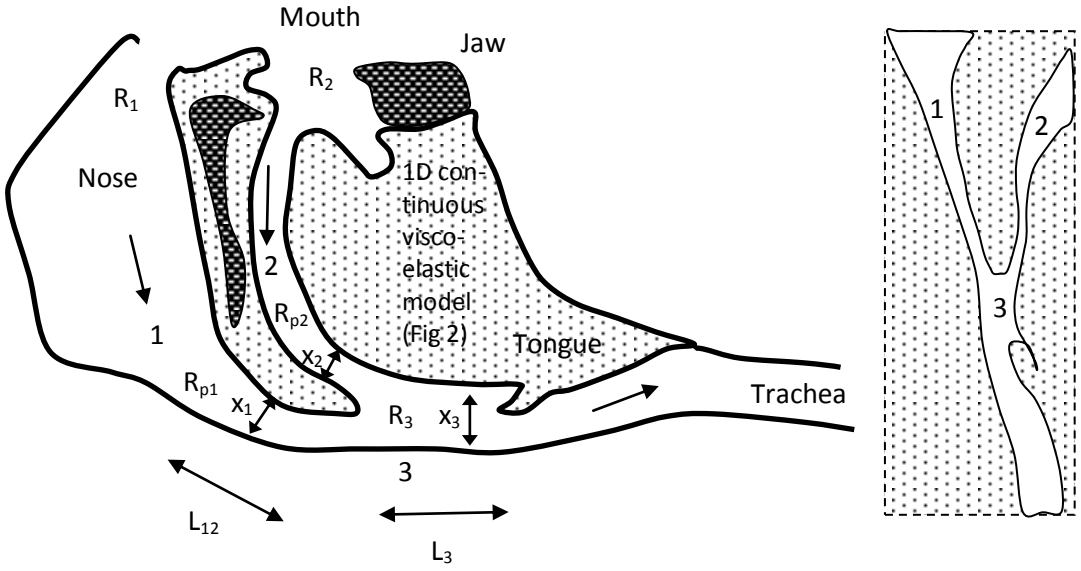

Figure 1. Simplified one dimensional model of the upper airway in a snorer. *Branched parallel channels through the nose (1) and mouth (2) are separated by the rigid, bony hard palate (darkly shaded) and the soft palate (lightly shaded). Channels 1 and 2 converge to a common oropharyngeal Channel 3 at the base of the tongue in a "Y-shaped" pattern (inset). Branches of the Y describe slit-like passages on the nasal and oral sides of the soft palate, when the palate is pushed posteriorly (down) by the tongue to form a wedge between the tongue surface and the posterior pharyngeal wall. The tongue (genioglossus muscle) suspended from the rigid jawbone (dark shading) acts as a continuous viscoelastic body. Critical time-varying distances, defining narrow points in the upper airways, are represented by the variables x_1, x_2, and x_3. Ohmic resistances of the component channels are denoted by constants R. R_1 is nose resistance. R_2 is mouth resistance. R_{p1} is the narrow soft palatal region of the nasal channel. R_{p2} is the narrow soft palatal region of the oral channel. Variables x_1 and x_2 sum to a constant value; that is, as x_1 decreases, x_2 increases and vis versa. Variable x_3, representing the distal common channel of the "Y", is independent of variables x_1 and x_2. The initial values of these variables at time zero (the beginning of calculations) represent equilibrium positions for any particular combination of gravity and muscle tone.*

In three dimensions the Channels 1, 2, and 3 are slit-like openings with a roughly common right-left width, s, of the slits and approximate axial lengths L_{12} for axial length of the narrows region of the soft palate, and axial length L_3 for common Channel 3. The relatively small widths of the slits in the narrow, flow-limiting regions of the three narrows channels are denoted x_1, x_2, and x_3 and defined in Figure 1. The width of the nasopalatal channel is defined as x_1. The width of the oropalatal channel is defined as $x_2 = x_{max} - x_1$. The sum of x_1 and x_2, equal to x_{max}, is constant owing to the shuttling of the palate in the wedge position over a small range of travel between the pharynx and the tongue. The width of common Channel 3 is denoted x_3.

Assuming laminar airflow, resistances of the channels can be calculated using the generalized Poiseuille Law for both circular and "racetrack shaped" cross sections (Appendix 1). The approximate nasal, oral, palatal, and oropharyngeal resistances are

$$R_1 = \theta\frac{8\pi\mu L_{nose}}{A_1^2} \quad R_2 = \theta\frac{8\pi\mu L_{mouth}}{A_2^2} \quad R_{p1} = \theta\frac{8\pi\mu L_{12}}{A_{p1}^2}, \quad R_{p2} = \theta\frac{8\pi\mu L_{12}}{A_{p2}^2}, \quad R_3 = \theta\frac{8\pi\mu L_3}{A_3^2}, \quad (3a)$$

where μ is the viscosity of air (0.00018 g/(cm-sec)), and where $0.5 < \theta \leq 1$ is a shape factor that depends on the degree of flattening or ovalization of the cross section of the passageway. For typical pharyngeal shapes $\theta \sim 0.6$. In terms of the slit-width variables x_1, x_2, and x_2, the approximate narrows resistances during snoring are

$$R_{p1} \approx 5\frac{\pi\mu L_{12}}{s^2 x_1^2}, \quad R_{p2} \approx 5\frac{\pi\mu L_{12}}{s^2 x_2^2}, \quad R_3 \approx 5\frac{\pi\mu L_3}{s^2 x_3^2}. \quad (3b)$$

The typically smaller nasal and oral resistances to airflow, R_1 and R_2 can be estimated from anatomical measurements in a similar way.

In the present discussion airflow is defined as positive in direction during inspiration and negative in direction during expiration. The major focus of the paper will be on the inspiratory phase when snoring and sleep apnea are most pronounced. In this case the total airflow is given by

$$i_{tot} = \frac{P_0 - P_{lung}}{R_{tot}}, \quad (4)$$

where P_0 is ambient or atmospheric pressure, and P_{lung} is alveolar pressure, as defined in classical respiratory physiology. Normally, $P_0 = 0$ (gauge pressure), in the absence of ventilator support, with $P_{lung} <$,0 during inspiration, and $P_{lung} > 0$ during expiration. Airflows in the branches of the Y, using standard expressions for flow in parallel resistive channels, are

$$i_1 = \frac{R_2'}{R_1' + R_2'} i_{tot} \quad \text{and} \quad i_2 = \frac{R_1'}{R_1' + R_2'} i_{tot}. \tag{5}$$

Note that when $R_2' >> R_1'$ nearly all air flows through Channel 1 and $i_1 \to i_{tot}$. When $R_1' >> R_2'$ nearly all air flows through Channel 2 and $i_2 \to i_{tot}$. When $R_1' = R_2'$, then $i_1 = i_2 = \frac{1}{2} i_{tot}$, as expected.

The Venturi effect

A major hypothesis underlying development of the present biomechanical model is that the palatal flutter is a consequence of pressure differences that develop between Channels 1 and 2 across the midpoint of the narrows region of the soft palate in response to differential airflow and the corresponding Venturi effects. The physics and mathematics of the Venturi effect are derived from first principles in Appendix 2. This effect happens when a fluid flows in a tube or conduit of varying diameter or cross section. For a constant or quasi-steady state flow (cm^3/sec), the axial velocity of the fluid (cm/sec), and in turn the kinetic energy of the fluid, which is proportional to axial velocity squared, is greater in the narrowed regions. By conservation of energy, the potential energy, which is related to pressure, must be less in the narrowed regions. Specifically, the Venturi effect is the reduced pressure that occurs when a fluid flows through a constricted section of a tube or pipe. The Venturi effect happens in the narrows regions of the sleeper's pharynx because of relatively high velocities of airflow through the narrowed regions.

As shown in Appendix 2 the added negative pressure that is created by fast moving air or gas in a single narrow channel can be calculated using the expression

$$\Delta P_v = -\frac{1}{2} \rho i^2 \left(\frac{1}{A_n^2} - \frac{1}{A_0^2} \right), \tag{6}$$

where ρ is the mass density of the fluid, i is the volume flow (cm^3/sec), A_n is the cross sectional area of the narrow channel where P_v is measured, and A_0 is the cross sectional area of a wider reference channel where flow velocity is not increased. Venturi pressures of this kind will feature prominently in the present theory of snoring and sleep apnea, together with the usual resistive or Ohmic pressures associated with airflow through narrow passageways.

Simplified model of the tongue

It is convenient first to determine how the width of common Channel 3 changes with Venturi and Ohmic pressures caused by airflow. For this task a model of the tongue is needed. Figure 2(a) shows a simplified one dimensional, continuous model of the tongue as a distributed mass that is fixed at the origin of the genioglossus muscle at the inner angle of the jaw near the midline and continues to the region of the oropharynx. The mass of the forwardly protruding part of the

tongue is omitted for simplicity, and only the genioglossus muscle is considered as being of biomechanical importance in the context of the present problem. The model, therefore, represents not the whole tongue, but only the column of muscle tissue extending from the jaw to the base of the tongue, which is shown horizontally in Figure 2. The goal is to determine the motion of the surface of the base of the tongue in the direction extending from the angle of the jaw toward the posterior oropharyngeal wall. It is this motion that tends to occlude the airway and is also characteristic of tongue base snoring [17].

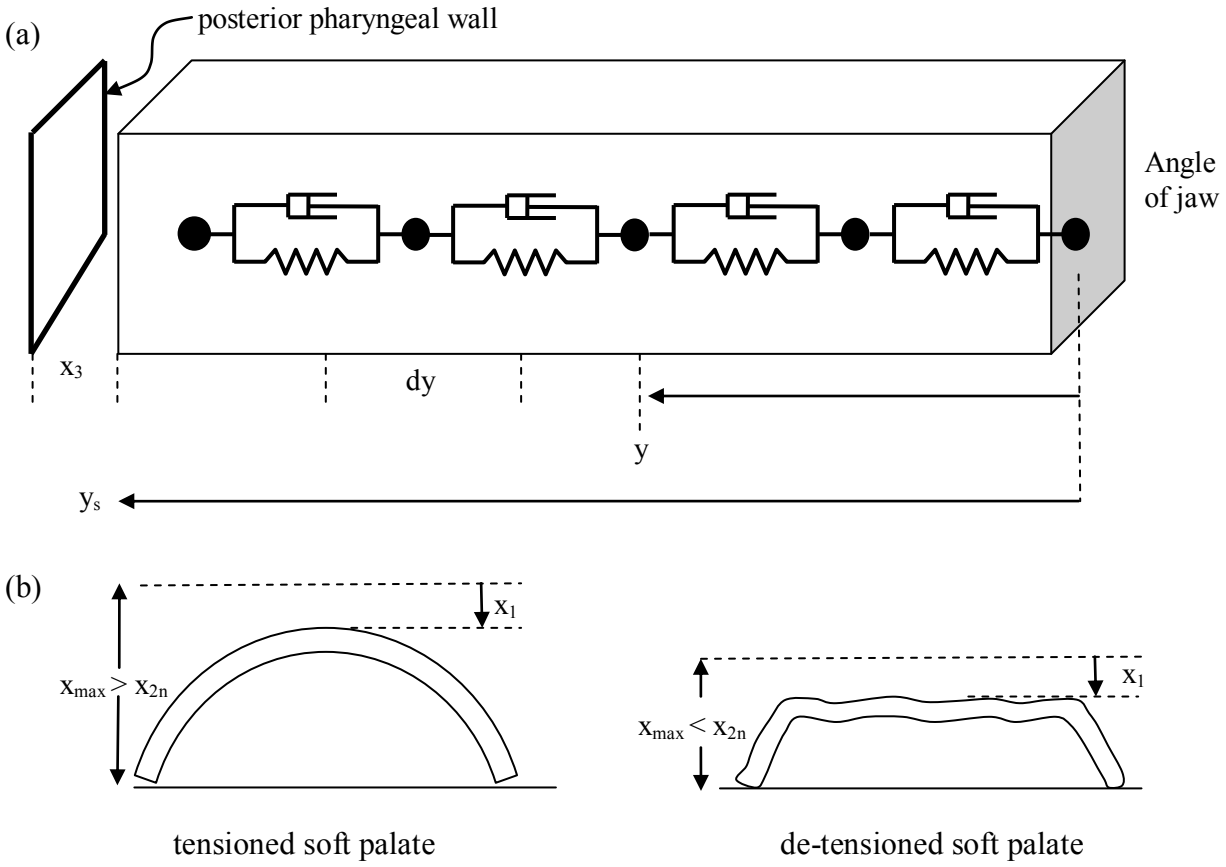

Figure 2. Models of tongue and soft palate. *(a) Continuous Voigt model of a viscoelastic tongue, composed of an arbitrary number of series mass elements, springs, and dampers. The cross section of the viscoelastic solid is A. For simplicity of drawing only four Voigt units are shown. (b) Model of the soft palate as an arch of constant curvature (sector of a cylindrical shell) having thickness, h, length, L_p, and unstressed radius, r_0. When the combined width of nasal and oral channels is greater than the unstressed, neutral value, x_{2n}, (left), the soft palate acts as a weak elastic band. When the combined width of nasal and oral channels is less than the unstressed, neutral value, x_{2n}, (right), the middle section of the soft palate acts as an unsupported plate-like mass. In numerical simulations both the unsupported soft palate and the (right) and the supported soft palate (left) can be modeled by assigning zero or nonzero values to associated spring and damping constants.*

Accordingly, the tongue is represented as a rectangular block of viscoelastic material, divided into an arbitrary number of differential slices, which are dy thick. The block has cross sectional area A, and unstressed length L_t. In turn, we can specify the spring constant for stretching or compression of the model for Young's modulus E_t of tongue muscle as $k = E_tA/L_t$. For the analogously defined damping modulus, D_t, the segmental damping constant $\mu = D_tA/L_t$. The mass density of the tongue is denoted ρ. The unstressed distance from the anchor point at the angle of the jaw to any particular point within the mass of the tongue denoted y. The pressure at the axial midpoint of Channel 3 acting on the surface of the tongue is denoted P_3. During inspiration a negative internal pressure, including Ohmic and Venturi pressures, in Channel 3 exerts a positive or extending force in the y-direction on the base of the tongue, making the tongue longer. The time-varying distance from the angle of the jaw to the surface of the base of the tongue is denoted $y_s(t)$.

The function $y_s(t)$ is determined by the balance of the pressure in Channel 3 acting on the surface of the tongue and the reactive spring and damping forces from compression or stretching of the tongue tissue. For low frequencies of oscillation, ignoring strain waves within the substance of the tongue, and assuming uniform compression or stretching of the viscoelastic material, the acceleration of a thin slice of thickness, dy, of tongue tissue at level y of the model is

$$\ddot{y} = \ddot{y}_s \frac{y}{L_t}. \tag{7}$$

Invoking Newton's second law, the total force acting on the tongue surface equals the total mass times acceleration in the y-dimension of the entire model, including the sum of the interior element masses and accelerations. The mass at any level, y, is $\rho A dy$. Then, letting Δ represent the change in length of the model (positive change = extension) and noting that velocity $\dot{\Delta} = \dot{y}_s$ and acceleration $\ddot{\Delta} = \ddot{y}_s$, we have

$$-P_3A - \frac{EA}{L_t}\Delta - \frac{DA}{L_t}\dot{\Delta} = \int_0^{L_t}\left(\ddot{\Delta}\frac{y}{L_t}\right)(\rho A dy) = \frac{\rho A\ddot{\Delta}}{L_t}\int_0^{L_t} y dy = \frac{\rho A\ddot{\Delta}}{L_t}\frac{L_t^2}{2}. \tag{8}$$

This is an equation of motion for the acceleration, $\ddot{\Delta}$, of the surface of the tongue. The coefficient of acceleration in Equation (8), that is, the effective mass of the tongue in this setting, is one half the total mass of the tongue or

$$m_e = \frac{\rho A L_t}{2}. \tag{9}$$

Rearranging and simplifying, the equation of motion for the surface of the base of the tongue becomes

$$\ddot{\Delta} + \frac{2D}{\rho L_t^2}\dot{\Delta} + \frac{2E}{\rho L_t^2}\Delta = -\frac{2P_3(t)}{\rho L_t}. \quad (10)$$

The change in position of the top surface of the tongue can be computed from suitable initial conditions for successive small time steps, Δt, by numerical integration. For example, using the simple Euler method,

$$\dot{\Delta}(t + \Delta t) = \dot{\Delta}(t) + \ddot{\Delta}(t)\Delta t \quad (11)$$

$$\Delta(t + \Delta t) = \Delta(t) + \dot{\Delta}(t)\Delta t\,. \quad (12)$$

Here a numerical method is used because the function $P_3(t)$ is not a simple sinusoidal function, necessarily, and depends on multiple parameters of the complete upper airway model. The width of Channel 3 between the base of the tongue and the posterior pharyngeal, $x_3(t)$, wall can then be computed from the initial unstressed width, $x_3(0)$, and the change in position of the top surface of the tongue,

$$x_3 = x_3(0) - \Delta\,. \quad (13)$$

The boundary condition that the tongue is not allowed to penetrate the opposite posterior pharyngeal wall can be implemented according to the following pseudocode for an inelastic collision:

```
if x3 < 0 Then {
        x3 = 0
        Δ̇ = 0
        Δ = x3(0)
}
```

Simplified model of the soft palate

During normal breathing in the awake state the soft palate can be seen through the open mouth as a partial arch (Figure 2(b) left) supported by the anterior and posterior tonsillar pillars, including the palatoglossus and palatopharyngeus muscles, extending from the tongue and lateral edges of the pharyngeal wall, respectively. The soft palate is also supported from above and laterally by the smaller tensor veli palatine muscles on each side. In the awake state the palate can be modeled as a partial arch of constant curvature, as described in Appendix 3, with the mid portion of the free edge of the soft palate constrained by a spring, representing lumped supporting muscles and soft tissues on each side and characterized by a ratio of spring constant, k, to area, A, $\frac{k}{A} = \frac{Eh}{r_0^2}$, where E and h are the Young's modulus of elasticity and thickness of the palatal arch tissue, and r_0 is the radius of curvature of the arch. For viscoelastic models the

corresponding ratio of damping constant to area $\frac{\mu}{A} = \frac{Dh}{r_0^2}$. This model of the soft palate applies to the awake state during normal breathing, either with the mouth open or with the mouth closed. To model the unsupported palatal arch the corresponding values of k and μ can be set to zero, if desired.

However, during sleep and snoring with relaxation of the tongue muscle, the palatal arch becomes flattened and constrained between the tongue and the posterior pharyngeal wall. A key assumption of the present model is that this entrapment of the soft palate essentially de-tensions the middle portion of the free edge of the soft palate near the uvula. In this state the soft palate undergoes bending deformation but not stretching deformation. The forces required for bending deformation are substantially less than the forces required for stretching deformation. This principle can be demonstrated by anyone, quite simply, using a rubber band or a green leaf. Accordingly, during snores the de-tensioned soft palate acts essentially as a simple, unsupported mass in response to the pressure difference between the nasal side and the oral side of the narrows region of the soft palate (Figure 2(b) right).

In particular, if x_{2n} represents the unstressed or neutral position distance between the narrows region of the soft palate and the tongue (see Figure 2(b)), and if the combined distance $x_{max} = x_1 + x_2$ is less than x_{2n}, then the elastic forces represented by the spring constant, k, equal zero, and, in turn, $k/A = 0$, and similarly the damping factor $\mu/A = 0$. The anatomic values for x_{2n} can vary greatly, as described by the Mallampati Classification [18]. For purposes of modeling the awake state the restoring force/area, F/A, on the soft palate provided by the palatal arch can be specified as follows: If $x_{max} > x_{2n}$ then $F/A = k(x_{max} - x_{2n} - x_1) - \mu\, dx_1/dt$ for x_1 = distance between the soft palate and posterior pharyngeal wall in Figure 2, as before. However, if $x_{max} < x_{2n}$, then $F/A = 0$. For most stimulations of snoring and sleep apnea presented here the normalized reactive forces exerted by the palatal arch, F/A, are zero.

Pressures acting on the soft palate

To create a simple one dimensional model of palatal snoring one may begin by specifying pressures at the midpoints of Channels 1 and 2 in the narrows region of the upper airways. As shown in Appendix 2, these pressures, including resistive (Ohmic or "iR") drop and Venturi effects are

$$P_1 = P_0 - i_1\left(R_1 + \frac{R_{p1}}{2}\right) - \frac{1}{2}\rho_{air} i_1^2\left(\frac{1}{A_{p1}^2} - \frac{1}{A_1^2}\right) \quad \text{and} \tag{14}$$

$$P_2 = P_0 - i_2\left(R_2 + \frac{R_{p2}}{2}\right) - \frac{1}{2}\rho_{air} i_2^2\left(\frac{1}{A_{p2}^2} - \frac{1}{A_2^2}\right), \tag{15}$$

where ρ_{air} is the density of air, A_{p1} is the narrow cross section of Channel 1 near the soft palate, A_1 is the relatively wide cross section of the nose, A_{p2} is the narrow cross section of Channel 2 near the soft palate, and A_2 is the relatively wide cross section of the partially open mouth.

The driving force of palatal snoring is provided by the trans-palatal pressure difference $\Delta P = P_1 - P_2$ in the narrows region. Positive ΔP makes variable x_1 bigger, pushing the palate away from the posterior pharyngeal wall, toward the tongue. Negative ΔP makes variable x_1 smaller, pulling the palate away from the tongue and toward the posterior pharyngeal wall. Interestingly, the Venturi effect for parallel channels is greater on the side of greater flow, not the side of smaller width. If x_1 is $< x_{max}/2$, then $i_2 > i_1$. Larger i_2 makes P_2 more negative, pushing the palate toward the centerline. If x_1 is $> x_{max}/2$, then $i_1 > i_2$. Larger i_1 makes P_1 more negative, again pulling the palate toward the centerline. Thus the palate has a stable mid position, like a pendulum, but is free to oscillate about this equilibrium. Note that incorporation of parallel flow channels, rather than a single channel is critical for describing this effect, and in turn, palatal flutter.

Equation of motion for the soft palate

To the extent that the curvature of the free edge of the soft palate is greater than the curvature of the base of the tongue or posterior pharyngeal wall, the palate will be de-tensioned in the wedge position. Accordingly, a major simplifying assumption of the present model is that for practical purposes the soft palate acts as a simple mass during snoring. Of course, the soft palate remains tethered in the axial dimension (perpendicular to the direction of flutter) by its attachment to the hard palate anteriorly. Thus it is effectively suspended by the hard palate against gravity in the supine position. However, the free edge of the soft palate in the narrows region is freely movable in the orthogonal dimension between the tongue and posterior pharynx (Figure 1).

Further, as observed by Trudo et al. [19], the lateral diameter of pharynx tends to shrink during inspiration, in association with negative airway pressures, especially in heavy snorers [20]. This anatomic change further de-tensions the suspensory tissues of the soft palate during sleep, allowing the soft palate (or a substantial portion of the soft palate near its free edge) to act as an unsupported flat mass that moves in response to the time-varying pressure difference, $\Delta P(t)$, between the nasopharynx and oropharynx [14].

Hence, unless otherwise specified, we shall regard the free edge of the soft palate as a mass of surface area, A, thickness, h, and density, ρ. Applying Newton's second law of motion (force = mass × acceleration) we have $A\Delta P = \rho A h \ddot{x}_1$, where ΔP is the trans-palatal pressure difference just derived. In turn, the one dimensional model of the palate can be solved numerically for successive small, discrete time steps, Δt, starting with suitable initial conditions, as

$$\ddot{x}_1 = \frac{\Delta P}{\rho h} \tag{16}$$

$$\dot{x}_1 = \dot{x}_1 + \ddot{x}_1 \Delta t \tag{17}$$

$$x_1 = x_1 + \dot{x}_1 \Delta t\,. \tag{18}$$

In the event that it is desired to compute motion of the soft palate for cases such as the awake state having non-negligible stiffnesses or damping properties, represented by spring and damping constants, k and μ, it is only necessary to upgrade the expression for palatal acceleration to $\ddot{x}_1 = \frac{\Delta P}{\rho h} - \frac{\mu}{A}\dot{x}_1 - \frac{k}{A}x_1$, with suitable attention to boundary conditions, and proceed numerically as before. The tongue and pharyngeal wall boundary conditions for inelastic collisions with the soft palate can be implemented according to the following pseudocode:

```
if x1 ≤ 0 Then {
        x1 = 0
        ẋ1 = 0
}

if x1 > xmax Then {
        x1 = xmax
        ẋ1 = 0
}
```

Complete palate and tongue model

The palate and tongue models can be combined to describe the critical tissue dynamics of snoring and sleep apnea in terms of palatal motion (x_1 vs. time) and in terms of the gap between the base of the tongue and the pharyngeal wall (x_3 versus time). These dynamics can be investigated as functions of model parameters and constants that describe various anatomic and physiologic states. Box 1 gives the sequence of calculations for the resulting mathematical model of snoring and sleep apnea. The multiple parameters are all defined on the basis of physics, anatomy, and physiology. There are no free parameters or arbitrary constants.

Box 1: a first-principles mathematical model of snoring and sleep apnea

Define

ρ soft tissue density
ρ_{air} air density
μ air viscosity
R_1 nasal resistance
R_2 mouth resistance
R_{aw} airway resistance
dt time step for integration
E Young's modulus of tongue muscle
A_1 nose reference cross section
A_2 mouth reference cross section
$x_3(0)$ initial common channel width
x_{max} total palatal channel width
P_0 ambient air pressure
P_{lung} lung pressure
L_{12} soft palate narrows length
L_3 oropharynx narrows length
h soft palate thickness
L_t tongue length
s span of palate pharynx
θ airway cross section shape factor
$x_1(0)$ initial position for x_1
D damping modulus of tongue muscle

Compute

Δ change in tongue base position from model of tongue, Equation (12)

$x_3 = x_3(0) - \Delta$ base of tongue position as a function of time, Eq. (13)

$A_{p1} = sx_1$, $A_{p2} = s(x_{max} - x_1)$, narrows areas near soft palate

$A_3 = sx_3$ oropharyngeal area of Channel 3

$R_1 = \theta \frac{8\pi\mu L_{nose}}{A_1^2}$, $R_2 = \theta \frac{8\pi\mu L_{mouth}}{A_2^2}$ nose and mouth resistances

$R_{p1} = \theta \frac{8\pi\mu L_{12}}{A_{p1}^2}$, nasal side narrows resistance

$R_{p2} = \theta \frac{8\pi\mu L_{12}}{A_{p2}^2}$, oral side narrows resistance

$R_3 = \theta \frac{8\pi\mu L_3}{A_3^2}$, common channel resistance

$R_1' = R_1 + R_{p1}$, $R_2' = R_2 + R_{p2}$ lumped nose and mouth resistances

$R_{tot} = \frac{R_1' R_2'}{R_1' + R'} + R_3 + R_{aw}$ total resistance

$i_{tot} = \frac{P_0 - P_{lung}}{R_{tot}}$ total airflow

$i_1 = \frac{R_2'}{R_1' + R_2'} i_{tot}$ and $i_2 = \frac{R_1'}{R_1' + R_2'} i_{tot}$ nose and mouth channel airflows

$P_1 = P_0 - i_1\left(R_1 + \frac{R_{p1}}{2}\right) - \frac{1}{2}\rho_{air} i_1^2 \left(\frac{1}{A_{p1}^2} - \frac{1}{A_1^2}\right)$ pressure on nasal side of soft palate

$P_2 = P_0 - i_2\left(R_2 + \frac{R_{p2}}{2}\right) - \frac{1}{2}\rho_{air} i_2^2 \left(\frac{1}{A_{p2}^2} - \frac{1}{A_2^2}\right)$ pressure on oral side of soft palate

$\Delta P = P_1 - P_2$ trans-palatal pressure difference

$\ddot{x}_1 = \frac{\Delta P}{\rho h}$, $\dot{x}_1$ x_1 acceleration, speed and position of soft palate position as a function of time

Parameter values

Anatomic dimensions (Table 1) were estimated from abundant CT and MRI images freely available on the Internet, combined with standard adult head dimensions. Anatomic dimensions of the airway do vary with inspiratory pressure [13, 19]. For the purpose of the present model, however, these changes are accounted for in the selection of "time zero", which unless otherwise specified represents the midpoint of inspiration. That is, the models and simulations represent mid-inspiratory state when snoring or airway occlusion is most likely to occur. For this state the internal airway dimensions are considered to be already narrowed in accordance with prevailing negative lung pressures. The focus is on what happens next. Only motions of the soft palate and base of the tongue are analyzed in detail.

Table 1: anatomic dimensions for the standard normal model

Anatomic dimension	**Value**
Average right-left width of the internal nares on each side, accounting for the presence of turbinate bones	0.25 cm
Average height of the internal nares on each side	2.4 cm
Average front to back length of the inner nose, L_{nose}	9 cm
Short cross sectional dimension of nasopharynx	0.5 cm
Long cross sectional dimension of nasopharynx	2.0 cm
Length of nasopharynx	2.5 cm
Width of oropharynx before narrows region for computation of R_2	0.5 cm
Right-left dimension of oropharynx	4.0 cm
Length of oropharynx	7.0 cm
Soft palate narrows length, L_{12}	1.5 cm
Oropharynx narrows length, L_3	2 cm
Soft palate thickness, h	0.3 cm
Length of tongue from mandible to oropharyngeal surface, L_{mouth}	9 cm
Side to side width of naso- and oropharyngeal channels, s	4 cm
The ratio of total palatal channel width ($x_1 + x_2$, the short cross sectional dimension) to common oropharyngeal channel width	1
Shape factor, θ, for upper airway cross sections as flattened ovals	0.6

Additional model parameters are given in Table 2 and in Table 3.

Table 2: standard parameter values

Symbol	Numerical value	Units	Definition
R_1	0.04072	dyne-sec/cm^5	nasal resistance computed from dimensions in Table 1
R_2	0.00475	dyne-sec/cm^5	mouth resistance computed from dimensions in Table 1
R_{aw}	2.66	dyne-sec/cm^5	airway resistance (tracheal to alveoli)
dt	0.000001	sec	time step for integration
E_{tongue}	100000	dynes/cm^2	Young's modulus of tongue muscle (fully relaxed)
E_{tongue}	600000	dynes/cm^2	Young's modulus of tongue muscle (moderate muscle tone)
A0	5	cm^2	nose/mouth reference cross section
x3(0)	0.1	cm^2	initial common channel width in cm for simulations of palatal snoring
x_{2n}	1.5	cm	unstressed and uncrimped neutral position of soft palate
P_0	0	dynes/cm^2	ambient gauge pressure
P_{lung}	-1333	dynes/cm^2	lung pressure during inspiration
startRatio	various		initial position $x(0)/x_{max}$ = $x(0)/(alpha*x_3(0))$
k_Apalate	750	dynes/cm^3	Young's modulus / area of soft palate
ε	0.01	sec	ratio of damping modulus o Young's modulus of palate in sec
D_{tongue}	100	dyne-sec/cm^2	damping modulus of tongue muscle

Numerical values for Young's modulus of various soft tissues in the upper airway were based on published literature (Table 3). The reported stiffness values of skeletal muscle, including the tongue, vary widely, especially between relaxed and contracted states. Mid range, nominal values for Young's modulus of the tongue, for purposes of the present analysis and simulations, were taken as 10kPa in the relaxed state (low muscle tone, deep sleep), 60kPa for the awake and contracted state, and 30 kPa for the intermediate state representing partial arousal from obstructive sleep apnea. Upper airway resistance values were estimated from anatomic considerations based on head CT scans (Table 1) using Poiseuille's Law for laminar flow.

Table 3. Literature values for Young's modulus of soft tissues surrounding upper airways

Tissue	Young's modulus (Pa) middle value	Reference
Soft palate	900	Birch 2009 [21]
Soft tissues	1600	Chen 1996 [22]
Soft palate	7800	Cheng 2011 [23]
Tongue	15000	Payan 1998 [24]
Tongue in vivo*	10000	Brown 1985 [25]
Tongue passive	6000	Huang 2007 [26]
Posterior pharyngeal wall#	7800	Gavriely 1993 [27]
Relaxed skeletal muscle	16000	Shinohara 2010 [28]
Contracted skeletal muscle	100000	Shinohara 2010 [28]
Relaxed muscle	6200	Duck 1990 [29]
Fat tissue	2000	Comley 2010 [30]
Fat tissue	18000	Krauskop 1998 [31]

*estimated assuming rectangular box model, pharyngeal diameter 1.0 cm, tongue length 10 cm

estimated assuming wall tissue thickness is 1.0 cm

Analytical Results

Before proceeding to numerical calculations it is useful and insightful to solve some simplified test cases analytically. Studying the equations of the complete palate and tongue model in this way led to the discovery of multiple mechanisms of snoring. These include several types of palatal snoring and several types of base of tongue snoring.

Double sided palatal snoring with mouth open

The first such mechanism may be called double sided palatal snoring. This idealized test case represents a common form of normal snoring without significant airway obstruction. The nose and mouth are both open, and air flows over both sides of the soft palate. In this normal scenario the open nose and mouth areas A_1 and A_2 are large with respect to narrows areas A_{p1} and A_{p2}. The upper airways between the outside world and the narrows region of the soft palate contribute minimally to total airway resistance, so that $R_1 \approx 0$, $R_2 \approx 0$. Further, in the absence of severe airway obstruction by the base of the tongue, the width of common Channel 3 is approximately equal to the unstressed value, $x_3(0)$, and is nearly constant. The palate moves back and forth, so that as A_{p1} increases, A_{p2} decreases. The total cross section for airflow on both sides of the palate remains constant and is non-obstructing compared to airway resistance, R_{aw}. As a result, the values of R_{tot} and i_{tot} are approximately constant for any particular level of inspiratory lung pressure, $P_{lung} < 0$.

Under theses simplifying assumptions the mathematics of Box 1 becomes tractable for algebraic solutions. The pressures,

$$P_1 = P_0 - i_1\left(R_1 + \frac{R_{p1}}{2}\right) - \frac{1}{2}\rho_{air} i_1^2\left(\frac{1}{A_{p1}^2} - \frac{1}{A_1^2}\right) \tag{19}$$

and

$$P_2 = P_0 - i_2\left(R_2 + \frac{R_{p2}}{2}\right) - \frac{1}{2}\rho_{air} i_2^2\left(\frac{1}{A_{p2}^2} - \frac{1}{A_2^2}\right), \tag{20}$$

become

$$P_1 \approx P_0 - i_1\left(\frac{R_{p1}}{2}\right) - \frac{1}{2}\rho_{air} i_1^2\left(\frac{1}{A_{p1}^2}\right) \text{ and } P_2 \approx P_0 - i_2\left(\frac{R_{p2}}{2}\right) - \frac{1}{2}\rho_{air} i_2^2\left(\frac{1}{A_{p2}^2}\right). \tag{21}$$

Further, since

$$i_1 = \frac{R_2'}{R_1' + R_2'} i_{tot} \approx \frac{R_{p2}}{R_{p1} + R_{p2}} i_{tot} \quad \text{and} \quad i_2 = \frac{R_1'}{R_1' + R_2'} i_{tot} \approx \frac{R_{p1}}{R_{p1} + R_{p2}} i_{tot}, \tag{22}$$

we have

$$\begin{aligned} \Delta P \approx P_1 - P_2 &= \frac{1}{2}\rho_{air} i_2^2 \left(\frac{1}{A_{p2}^2} \right) - \frac{1}{2}\rho_{air} i_1^2 \left(\frac{1}{A_{p1}^2} \right) \\ &= \frac{1}{2}\rho_{air} i_{tot}^2 \left\{ \frac{R_{p1}^2}{\left(R_{p1} + R_{p2}\right)^2} \cdot \frac{1}{A_{p2}^2} - \frac{R_{p2}^2}{\left(R_{p1} + R_{p2}\right)^2} \cdot \frac{1}{A_{p1}^2} \right\} \end{aligned} . \tag{23}$$

Substituting for R_{p1} and R_{p2} in terms of the narrows cross sectional areas for Channels 1 and 2, A_{p1} and A_{p2}, with the same shape factors, θ, and simplifying leads to

$$\Delta P \approx \frac{1}{2}\rho_{air} \frac{A_{p2}^2 - A_{p1}^2}{A_{p2}^2 + A_{p1}^2} i_{tot}^2 . \tag{24}$$

Then expressing the areas in terms of span, s, and slit widths x_1 and $x_{max} - x_1$, and simplifying gives

$$\Delta P \approx \frac{1}{2s^2}\rho_{air} \frac{x_{max}^2 - 2x_{max}x_1}{\left(x_{max}^2 - 2x_{max}x_1 + 2x_1^2\right)^2} i_{tot}^2 . \tag{25}$$

This expression describes trans-palatal pressure, ΔP, as a function of the position of the soft palate, measured as distance x_1 from the posterior pharyngeal wall.

Figure 3 shows a specific numerical example of the trans-palatal pressure difference for this type of idealized double sided palatal snoring. In this example, the maximal gap, x_{max}, between soft palate surface and either opposing surface is 0.1 cm or 1 mm.

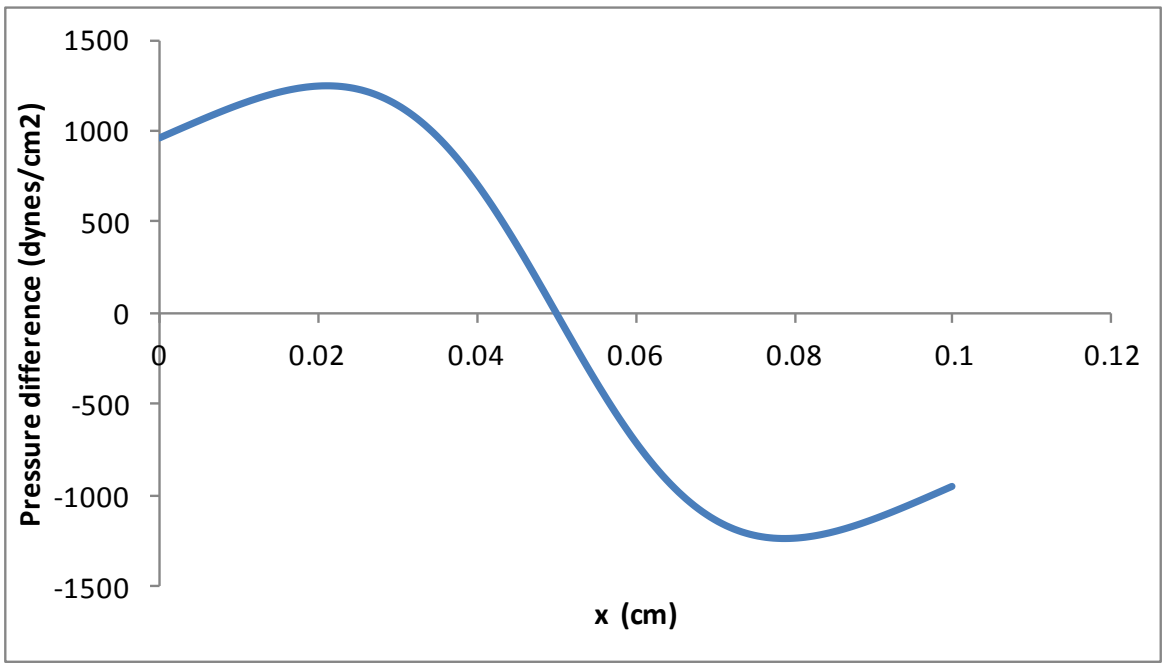

Figure 3. Pressure difference across the soft palate for idealized double sided palatal snoring, plotted as a function of variable x_1 , the position of the soft palate with respect to the posterior pharyngeal wall.

Note in Figure 3 that if $x_1 = x_{max}/2$, then $\Delta P = 0$. This is the neutral or equilibrium position. If $x_1 < x_{max}/2$, then $\Delta P > 0$, pushing the palate toward the neutral mid position at $x_{max}/2$. If $x_1 > x_{max}/2$, then $\Delta P < 0$, pulling the palate from the opposite side toward the neutral mid position at $x_{max}/2$. There is a roughly linear region of net Venturi pressure near the zero crossing point at $x_{max}/2$.

Further, by introducing the variable $u = x_1 - \frac{x_{max}}{2}$ to represent the displacement from the equilibrium position, the expression for the trans-palatal pressure difference more clearly represents the symmetry of the function about the zero crossing point. This expression as a function of u is

$$\Delta P \approx -4\frac{\rho_{air} i_{tot}^2}{s^2 x_{max}^3}\frac{u}{\left(1+4\frac{u^2}{x_{max}^2}\right)^2}. \qquad (26)$$

The function for ΔP is mirror-image symmetrical about $u = 0$. If $u > 0$ then the combined Venturi effects create a negative restoring force that reduces u. If $u < 0$ the combined Venturi effects create a positive restoring force that increases u. There is always a stable equilibrium.

The linear portion of the curve is described by the slope of $\Delta P(u)$ at $u = 0$, namely $-4\frac{\rho_{air} i_{tot}^2}{s^2 x_{max}^3} \equiv -c$, a constant.

The dependence of the trans-palatal pressure difference, ΔP, inversely on the cube of x_{max} is noteworthy. The phenomenon of this kind of double sided palatal snoring is highly dependent upon the total width of the air passages over and under the soft palate. Likewise, from the expanded expression for lumped constant, c, it is evident that trans-palatal pressure also increases directly as the square of total airflow, i_{tot}, which is related to respiratory effort and lung pressure, and inversely as the square of the right-to-left span, s, of the pharynx. Thus, the steepness of the curve in Figure 3 is strongly and non-linearly depended on several model parameters.

Exact solution for the small displacement case in symmetrical double sided palatal snoring

In the neighborhood of $u = 0$ the pressure difference is of the form $\Delta P \approx -cu$ for non-time-varying constant, $c = 4\frac{\rho_{air} i_{tot}^2}{s^2 x_{max}^3}$. For local cross sectional area, A, of the soft palate and tissue density, ρ, the equation of motion for the palate for small displacements from $u = 0$ is therefore

$$\Delta P A \approx -cuA = \rho A h \ddot{u}, \tag{27a}$$

or

$$\ddot{u} + \frac{c}{\rho h} u \approx 0. \tag{27b}$$

The physically meaningful steady-state solution to this classical second order differential equation for displacement, u, as a function of time, t, is $u = u_{max} \cos(\omega t)$, with angular frequency $\omega = \sqrt{\frac{c}{\rho h}}$, as is readily confirmed by differentiation. After an initial nonzero displacement, u_{max}, the system will oscillate with a natural frequency

$$f = \frac{1}{2\pi}\sqrt{\frac{4\rho_{air} i_{tot}^2}{s^2 x_{max}^3 \rho h}}. \tag{28}$$

This solution applies to cases with minimal damping, when the de-tensioned free edge of the soft palate moves essentially as a simple mass in the x_1 and x_2 dimensions, perpendicular to the palatal surface. As a numerical example, suppose that $\rho_{air} = 0.00122$ g/ml, $i_{tot} = 500$ ml/sec, $s = 4$ cm, $x_{max} = 0.1$ cm, $\rho = 1.0$ g/ml, and $h = 0.3$ cm. In this case we obtain a natural frequency, $f =$ 80 Hz. This value is very reasonable for common snoring.

The physics of the palate in a force field produced by Ventrui pressures on either side is analogous to the physics of a pendulum in the gravitational field at the Earth's surface or a simple spring and mass system. If the mass at the end of the pendulum or at the end of the spring is pulled in one direction, there will be a proportional restoring force directed toward the equilibrium position. If the mass is pulled in the opposite direction there will be an oppositely directed restoring force directed toward the equilibrium position. The equilibrium position for the mass is at the bottom of a potential energy well. With zero damping the oscillations will continue indefinitely. With some damping the oscillations will gradually die out, but the concept of the potential energy well nonetheless has utility in aiding understanding of the underlying mechanics.

Potential energy well for the soft palate in double sided snoring

Another way to visualize the biomechanics of idealized double sided palatal snoring is to plot the potential energy well associated with movement of the palate away from its neutral, equilibrium position at $x_{max}/2$. The potential energy is the work that must be done to move the palate from $x_1 = x_{max}/2$ to an offset position $x_1 \neq x_{max}/2$. The potential energy, U, per unit surface area of the palate is given by

$$\frac{U}{A} = \int_0^u -\Delta P(u)du = \int_0^u \frac{cu}{\left(1+\frac{u^2}{4x_{max}^2}\right)^2}du \ , \tag{29}$$

where $c = 4\frac{\rho_{air} i_{tot}^2}{s^2 x_{max}^3}$.

This expression for U/A can be integrated exactly as

$$U/A = 2cx_{max}^2\left(\frac{\frac{u^2}{x_{max}^2}}{1+4\frac{u^2}{x_{max}^2}}\right) \tag{30}$$

and is plotted in Figure 4..

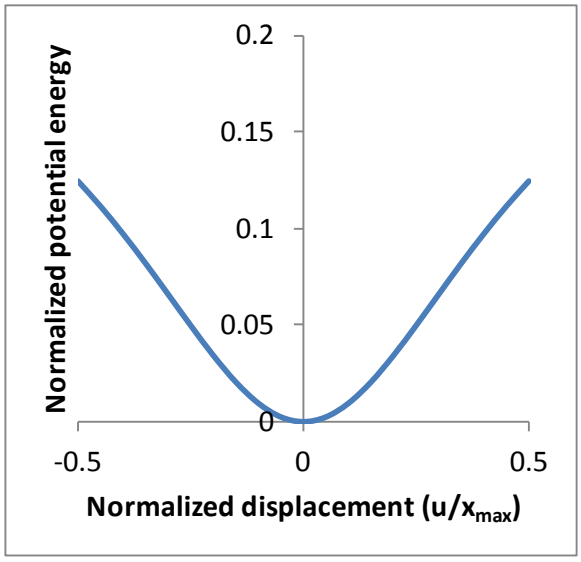

Figure 4. Potential energy well for double sided palatal snoring. *Normalized potential energy,* $\frac{U/A}{2cx_{max}^2}$*, is plotted as a function of normalized displacement* u/x_{max} *over the full range of* u *for a central equilibrium point at* $x_{max}/2$.

With the palate at neutral position, $x = x_{max}/2$, or $u = 0$ there is equal airflow occurs on both sides. The palate sits at the bottom of a potential energy well in a stable position, like a pendulum at rest. If the palate is moved by some force toward the tongue, $u > 0$, the space between palate and tongue is constricted, and there is less airflow on the tongue side and more airflow on the nasal side. The resulting imbalance in Venturi pressures creates a restoring force on the palate, which draws it back toward the midline, converting potential energy into kinetic energy. The palate does not stop at $u = 0$, because it has kinetic energy, like a pendulum. Instead the palate climbs the other side of the potential energy hill. Since it is acting essentially as a freely moving mass, with minimal damping or frictional energy loss, the posterior edge of the soft palate can continue to fluctuate around the equilibrium point at $u = 0$ for some time.

The depth of the potential energy well depends on the constant, $c = 4\frac{\rho_{air} i_{tot}^2}{s^2 x_{max}^3}$, and in turn in a nonlinear way on total airflow, i_{tot}, and combined channel dimensions x_{max}, and s. The greater the inspiratory airflow and the smaller the channel dimensions, the greater the Venturi pressures. Between breaths, when airflow is zero, the palate will continue moving for a time and likely settle at some off-center position along its course of travel. The stopping position may be random or may be biased at $u < 0$, owing to gravity in the supine position or to small tissue elastic forces between breaths. As the next inspiratory effort happens, positive inward airflow, i_{tot}, increases. The potential energy well reforms, and the palate, if positioned anywhere off center, will begin to oscillate again like a pendulum. As the inspiratory airflow increases toward

its physiologic peak value, the potential energy well deepens, adding energy to the system and offsetting small viscous losses. Hence snoring continues. This is why palatal flutter happens. With some damping the oscillations will gradually die out between breaths, as shown in subsequent numerical results. However the concept of the potential energy well still applies.

Single sided palatal snoring with mouth closed

As described by Quinn, Liistgrow and their coworkers [8, 17] using endoscopy in human subjects, palatal motion can also occur with the mouth completely closed. This observation suggests the existence of other modes of snoring, in which airflow passes over the nasal side of the palate only. One such mechanism, suggested by the present mathematics, may be called single sided palatal snoring. As before, in an idealized case the nasal passages are relatively unrestricted with $R_1 \approx 0$. However, with the mouth closed $R_2 \to \infty$. As with normal double sided palatal snoring, let us assume temporarily that the resistance of the common narrows passage at the base of the tongue is still small compared to total airway resistance, R_{aw}, and that $x_3 \approx x_3(0)$ and nearly constant. With zero airflow through the mouth, the airflow though Channel 1 between the palate and the posterior pharyngeal wall is the same as total airflow, i_{tot}.

The pressure P_2 on the oral side of the palate is most simply represented as

$$P_2 = P_{lung} + i_{tot} R_3 , \tag{31}$$

where R_3 is the resistance of the common channel at the base of the tongue, in this case approximately constant.

The pressure on the nasal side of the soft palate at the midpoint of its axial length, L_{12}, is

$$P_1 = P_{lung} + i_{tot} R_3 + i_{tot} \frac{R_{p1}}{2} - \frac{1}{2} \rho_{air} i_{tot}^2 \left(\frac{1}{A_{p1}^2} - \frac{1}{A_1^2} \right). \tag{32}$$

The trans-palatal pressure

$$\Delta P = P_1 - P_2 = i_{tot} \frac{R_{p1}}{2} - \frac{1}{2} \rho_{air} i_{tot}^2 \left(\frac{1}{A_{p1}^2} - \frac{1}{A_1^2} \right). \tag{33}$$

With unobstructed nasal passages we have $A_1 >> A_{p2}$, so that

$$\Delta P \approx i_{tot} \left(\frac{R_{p1}}{2} - \frac{1}{2} \frac{\rho_{air} i_{tot}}{A_{p1}^2} \right). \tag{34}$$

Substituting

$$A_{p1} = sx_1,\ R_{p1} = \theta\frac{8\pi\mu L_{12}}{A_{p1}^2},\ R_3 = \theta\frac{8\pi\mu L_3}{s^2x_3^2},\ R_{tot} = R_{p1} + R_3 + R_{aw},\ \text{and}\ i_{tot} = \frac{P_0 - P_{lung}}{R_{tot}},$$

and simplifying leads to

$$\Delta P = c_0\left[\frac{\frac{c_1}{2}}{c_1 + c_2x_1^2} - c_3\frac{x_1^2}{\left(c_1 + c_2x_1^2\right)^2}\right]. \tag{35}$$

This expression gives trans-palatal pressure as a function of soft palate position, x_1, where constants $c_0 = P_0 - P_{lung}$, $c_1 = \theta\frac{8\pi\mu L_{12}}{s^2}$, $c_2 = R_3$, and $c_3 = \frac{\rho_{air}\left(P_o - P_{lung}\right)}{2s^2}$.

A plot of this function for a typical normal case is shown in Figure 5(a). Figure 5(b) shows the region around the zero crossing point on an expanded scale. Over most of the domain of x_1 the pressure is strongly negative, drawing the palate toward the posterior pharyngeal wall at $x_1 = 0$, except for a small range close to $x_1 = 0$ where the narrowness of the palatal gap reduces total airflow and, in turn, the Venturi effect. In this narrow zone close to the pharyngeal wall the negative pressure on the oral side of the palate during inspiration dominates, producing a net positive trans-palatal pressure towards the oral side of the palate.

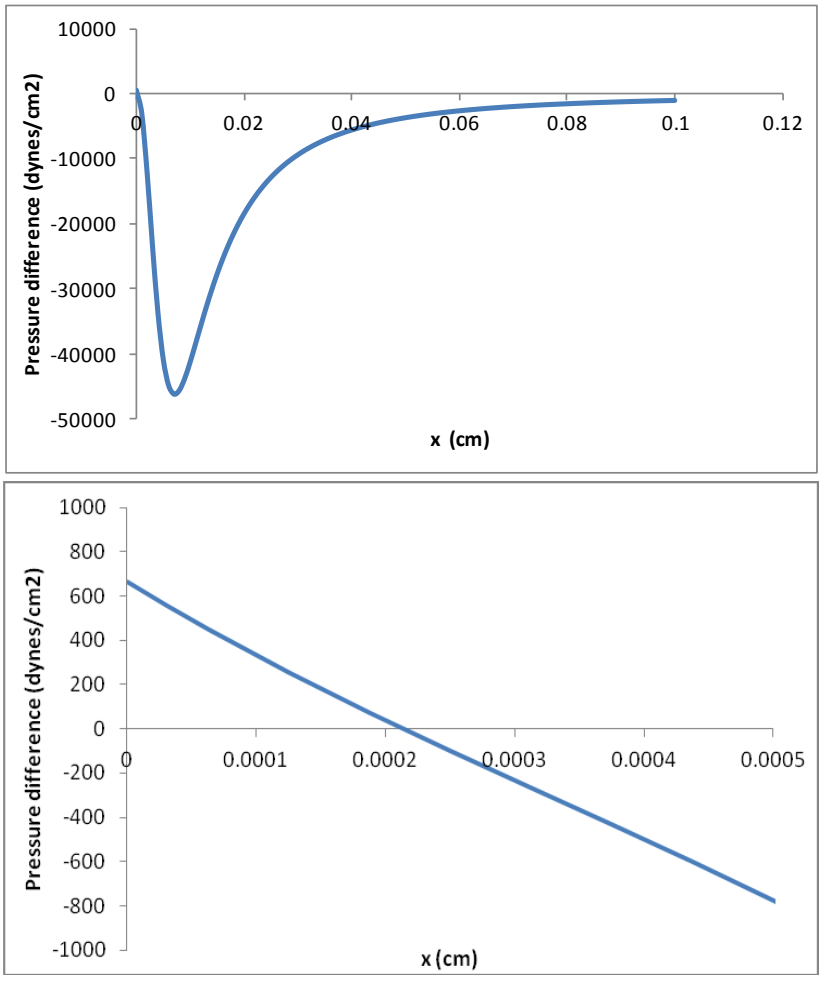

Figure 5. Pressure difference across the soft palate for single sided palatal snoring, plotted as a function of variable x_1, the position of the soft palate with respect to the posterior pharyngeal wall. *(a) full scale, (b) expanded scale in region of zero crossing point.*

The system exhibits a stable equilibrium at position, $\hat{x}_1$, when $\Delta P = 0$ and

$$\frac{c_1}{2} = c_3 \frac{\hat{x}_1^2}{c_1 + c_2 \hat{x}_1^2} \quad \text{or} \quad \hat{x}_1^2 = \frac{c_1^2}{2c_3 - c_1 c_2}. \tag{36}$$

Exact solution for the small displacement case in single sided palatal snoring

As before, we can define the displacement from the equilibrium position $u = x_1 - \hat{x}_1$, so that $x_1 = \hat{x}_1 + u$, and $x_1^2 = \hat{x}_1^2 + 2\hat{x}_1 u + u^2 \approx \hat{x}_1^2 + 2\hat{x}_1 u$ for $|u| << \hat{x}_1$ in the small signal case. In this case we have

$$x_1^2 \approx \hat{x}_1^2\left(1 + 2\frac{u}{\hat{x}_1}\right), \tag{37}$$

and using Equation (37) in Equation (35), we have the trans-palatal pressure as a function of u,

$$\Delta P \approx c_0 \frac{\frac{c_1}{2}}{c_1 + c_2\hat{x}_1^2\left(1 + 2\frac{u}{\hat{x}_1}\right)} - c_0 c_3 \frac{\hat{x}_1^2\left(1 + 2\frac{u}{\hat{x}_1}\right)}{\left(c_1 + c_2\hat{x}_1^2\left(1 + 2\frac{u}{\hat{x}_1}\right)\right)^2}. \tag{38}$$

In the vicinity of the equilibrium point, $\hat{x}_1$, the approximate slope

$$\frac{d(\Delta P)}{du} \approx -c_0 c_3 \frac{2\hat{x}_1}{\left(c_1 + c_2\hat{x}_1^2\right)^2} u \equiv -c' u, \tag{39}$$

a simple linear function of u (Figure 5(b)). Here c' is a lumped, non-time-varying constant. As was the case for double sided palatal snoring, the equation of motion for oscillations near the equilibrium point in single sided palatal snoring is therefore $\Delta P A \approx -c' u A = \rho A h \ddot{u}$, or

$$\ddot{u} + \frac{c'}{\rho h} u \approx 0. \tag{40}$$

The steady-state solution for small displacements, u, as a function of time, t, is $u = u_{max}\cos(\omega t)$, where the angular frequency $\omega = \sqrt{\frac{c'}{\rho h}}$. After an initial nonzero displacement u_{max} the system will oscillate with a natural frequency

$$f = \frac{1}{2\pi}\sqrt{\frac{c'}{\rho h}} = \frac{1}{2\pi}\sqrt{\frac{c_0 c_3}{\rho h} \cdot \frac{2\hat{x}_1}{\left(c_1 + c_2\hat{x}_1^2\right)^2}}. \tag{41}$$

Evaluating the various constants for a standard normal model (Tables 1, 2, and 3) gives a numerical value of f = 482 Hz, suggesting that single sided palatal snoring is higher frequency

than double sided palatal snoring. This type of snoring is easy for the author to simulate, as children sometimes do, to mimic the sound of a squealing pig. Although total resistance is high, there is still a small amount of inspiratory airflow, driven by a large inspiratory effort.

As shown in Figure 5, the equilibrium point is very close to the posterior pharyngeal wall (x_1 = 0) and far from mid-position ($x_{max}/2$). Since there is zero airflow through the mouth, there is physiologically significant restriction of airflow associated with single sided palatal snoring. Indeed, as shown in subsequent numerical results, this type of high pitched, squeaky snoring is a form of sleep apnea. Inspiratory airflow is very small.

Note in Figure 5(a) (extreme right) that when the separation of the soft palate from the posterior pharyngeal wall becomes greater than about 0.1 cm or 1 mm the Venturi pressure on the soft palate becomes very small. Such forces are predicted to exist in ordinary quiet breathing through the nose with the mouth closed. In this case one can speculate that the palate either adheres to the base of the tongue by a fluid seal and associated adhesive force (not formally modeled here) or alternatively is lifted very slowly off the tongue at a rate that changes dimension x_2 very little during the duration of inspiration, leaving the nasal Channel 2 open and unobstructed, as expected. This phenomenon can be seen in the movies of magnetic resonance images reported by Cheng and coworkers [32].

Base of tongue snoring

Base of tongue snoring was observed occasionally by Quinn and coworkers[17] using video endoscopy of instrumented sleeping subjects. This type of snoring was much less common than palatal snoring, but it is deserving of analysis, because under some circumstances it can transform into sleep apnea. To obtain an analytical model of pure base of tongue snoring consider a scenario in which Channels 1 and 2 remain close to normal caliber, but Channel 3 is selectively narrowed to a greater or lesser degree by retro-positioning of the base of the tongue toward the oropharyngeal wall—especially in the supine position. In this situation flow limitation may occur owing to Channel 3 narrowing only.

Although the posterior pharyngeal wall will move dynamically in response to Venturi pressures, the amount of movement is much less than the tongue, owing to the larger effective spring constant ($k = EA/L$) that is associated with the smaller effective length of posterior wall soft tissues, which are anchored ultimately by the spine, about 1 cm from the airway. This length is small compared to the effective length of the genioglossus muscle of the tongue, which is anchored to the midpoint of the mandible, about 10 cm from the airway in an adult human. For simplicity, therefore, we shall regard the posterior pharyngeal wall as a fixed reference plane in space and focus on the dynamic movement of the base of the tongue. (If it is desired to include effects of posterior wall motion in the narrowing of the Channel 3 airway, one can simply reduce the stiffness of the tongue by about 10 percent.)

The pressure at the axial midpoint in common Channel 3 between the posterior pharyngeal wall and the base of the tongue is

$$P_3 = P_{lung} + \frac{1}{2} i_{tot} R_3 - \frac{1}{2} i_{tot}^2 \frac{1}{s^2 x_3^2}. \quad (42)$$

Here

$$i_{tot} = \frac{P_0 - P_{lung}}{R_{tot}},\ R_{tot} = R_{12} + R_3 + R_{aw},\ R_{12} = \frac{8\pi\theta\mu L_{12}}{s^2 x_1^2 + s^2 (x_{max} - x_1)^2},\ R_3 = \theta \frac{8\mu L_3}{s^2 x_3^2}. \quad (43)$$

For cases of interest in which flow through Channels 1 and 2 is not limiting, one can assume a middle value for R_{12} with $x_1 = x_{max}/2$, and $x_{max} = \alpha x_3(0)$ for sizing factor, α, near 1. Then

$$R_{12} = \frac{8\pi\theta\mu L_{12}}{\alpha^2 s^2 x_3^2}. \quad (44)$$

After substitution and simplification, the axial midpoint pressure within Channel 3 can be written as

$$P_3 = P_{lung} + \frac{c_1}{c_2 x_3^2 + c_3} - \frac{c_4 x_3^2}{\left(c_2 x_3^2 + c_3\right)^2}, \quad (45)$$

where, using x_{30} as a shorter notation for $x_3(0)$ below,

$$c_1 = \frac{1}{2} \frac{8\pi\theta\mu L_3 P_{lung}}{s^2 x_{30}^2} \text{ in units of pressure x resistance} \quad (46)$$

$$c_2 = \frac{R_{aw}}{x_{30}^2} + \frac{16\mu L_{12} P_{lung}}{\alpha^2 s^2 x_{30}^4} \text{ in units of resistance / length}^2 \quad (47)$$

$$c_3 = \frac{8\pi\theta\mu L_3}{s^2 x_{30}^2} \text{ in units of resistance} \quad (48)$$

$$c_4 = \frac{\rho_{air} P_{lung}^2}{2 s^2 x_{30}^4} \text{ in units of pressure x resistance}^2 \text{ / length}^2. \quad (49)$$

As negative lung and Venturi pressures occur in Channel 3, they tend to draw the tongue toward the posterior pharyngeal wall and tend to reduce the width, x_3, of Channel 3. As progressive stretching of the tongue happens, reactive elastic forces pull the tongue away from the posterior pharyngeal wall and tend to increase the width, x_3, of Channel 3. The balance of these forces governs motion of the tongue and dynamic changes in x_3. In terms of pressures, the balance of forces/area in the positive direction of increasing x_3 is

$$F_{net} / A = \frac{E_t}{L_t}(x_{30} - x_3) - P_3, \text{ or} \tag{50a}$$

$$F_{net} / A = \frac{E_t}{L_t}(x_{30} - x_3) - \left[P_{lung} + \frac{c_1}{c_2 x_3^2 + c_3} - \frac{c_4 x_3^2}{\left(c_2 x_3^2 + c_3\right)^2} \right]. \tag{50b}$$

Here E_t is Young's modulus of the tongue, which could be in either a softer relaxed state (~ 10 kPa) or a stiffer higher tone state (~ 60 kPa), and L_t is the length of the tongue from the midpoint of the mandible to the oropharynx (~ 9 cm). Note that here the effect of gravity is included in the term x_{30} that reflects the state of stretch of the tongue at time zero of the simulation (typically mid-inspiration) including the balance of forces between gravity and the prevailing muscle tone and stiffness of the tongue. Hence gravity is not included specifically.

Figure 6(a) shows a plot of the resulting elastic force/area, intra-channel pressures, and the resulting difference function for a scenario of base of tongue snoring. The difference function is plotted in Figure 6(b) and on an expanded scale in Figure 6(c). In this example tongue muscle stiffness is 10 kPa (relaxed) and the unstressed tongue position is 0.6 cm (6 mm) from the pharynx. A stable zero crossing point occurs at values of x_3 near 0.5 cm. This point defines a stable equilibrium position, since as in other types of snoring, the slope of the function is negative at the zero crossing. If channel width, x_3, is greater than the zero crossing, the net force is negative, reducing channel width. If channel width is less than the zero crossing the net force is positive, increasing channel width.

However, if channel width is driven by muscle movement, gravity, or some other factor to a position much closer to the posterior wall at $x_3 < 0.05$ cm, then the net force becomes strongly negative, driving the surface of the tongue toward the posterior pharyngeal wall at position $x_3 = 0$. Very close to the wall there is another negatively sloping zero crossing near 0.0025 cm. This point indicates a stable equilibrium associated with very high resistance to airflow, effectively producing effort-independent sleep apnea. Thus once the tongue gets forced closer to the posterior pharyngeal wall than about one half millimeter, the physical forces will drive the tongue to a position that is almost, but not quite flush against the wall, blocking the airway. In this position the tongue is trapped in another potential energy well from which it is very difficult to escape. The result is base of tongue sleep apnea.

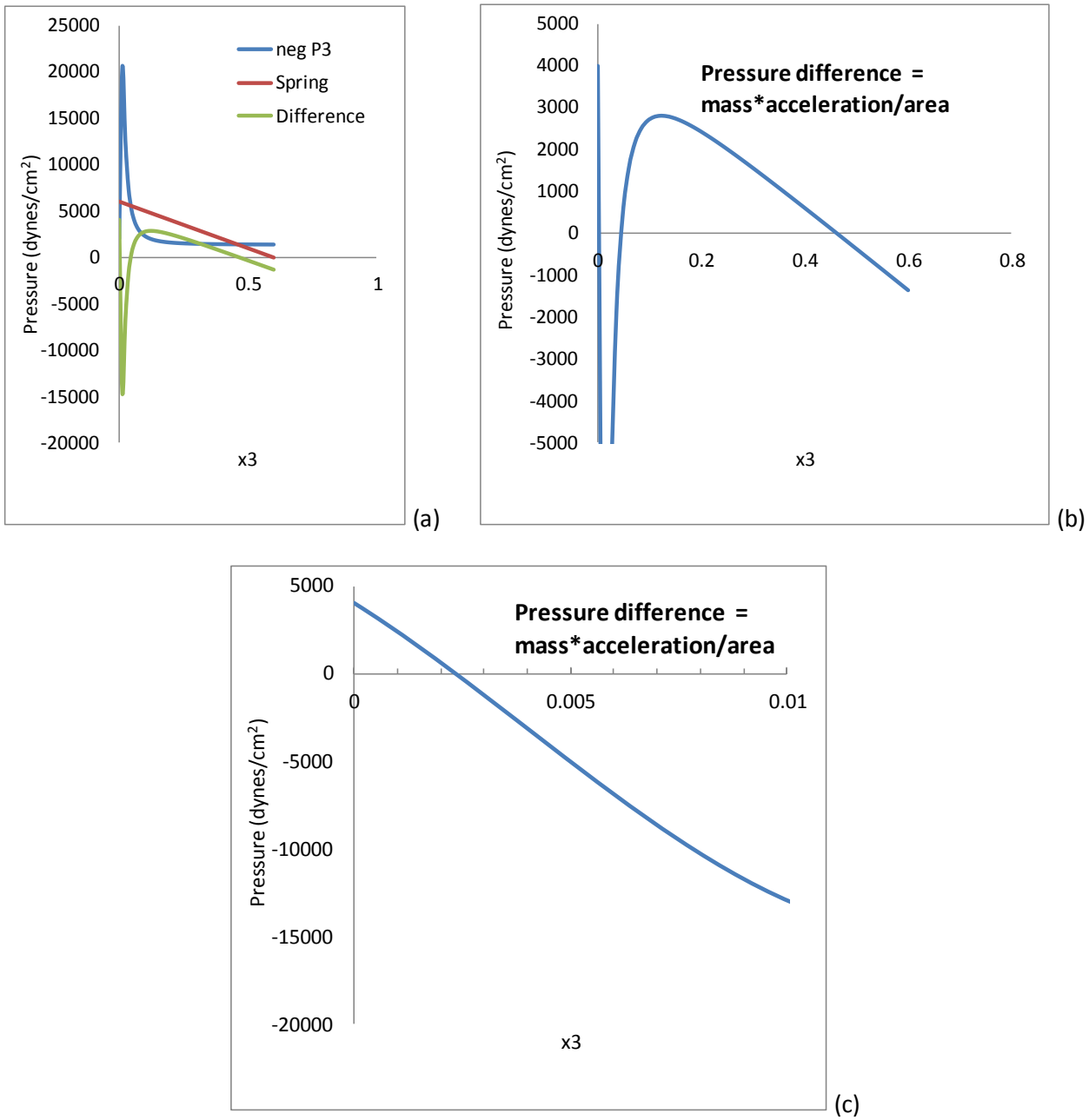

Figure 6. Force/area curves for base of tongue snoring with zero crossing points. *(a) absolute values at full scale; negP3 denotes the absolute value of the intraluminal pressure; Spring denotes the absolute value of reactive elastic effects of the tongue; Difference denotes net pressure on the tongue. (b) pressure difference at full scale, (c) expanded scale near zero showing a stable "apnea" crossing point. Distance x_3 is in units of cm.*

When x_3 is greater than either the near equilibrium point or the far equilibrium point the net force/area acting on the surface of the tongue is negative, a closing pressure, and the tongue is moves toward the pharynx. When x_3 is less than either equilibrium point the net force/area is positive, an opening pressure, and the tongue is moves away from the pharynx. In both cases there is a linear range of the net force/area in the neighborhood of the crossing point, $\hat{x}_3$. The approximately linear relation of net force vs. base of tongue position found in the present study is very similar to that described by Gavriely and Jensen [27] for a pharyngeal collapse model (their Figure 2), confirming the underlying biomechanics of whole tube wall oscillations. As the slit width becomes less than the critical width, the wall acceleration is positive, expanding the slit. As the slit width becomes greater than the critical width, wall acceleration becomes negative, collapsing the slit. In the absence of heavy damping , this state of affairs produces stable oscillations in slit width, in particular, base of tongue snoring.

The roughly constant slopes near the equilibrium points for base of tongue snoring mean that one can introduce the variable $u = x_3 - \hat{x}_3$, as before, to represent the displacement from a particular equilibrium position. Then the net force/area can be written as $F_{net} / A \approx -c''u$ for non-time varying constant, $-c''$, representing the local slope. The equation of motion for the tongue, with effective mass $m_e = \frac{\rho A L_t}{2}$ (from Equation (14)) is therefore

$$\Delta P A \approx -c''uA = \frac{\rho A L_t}{2}\ddot{u}, \tag{51}$$

or

$$\ddot{u} + \frac{2c''}{\rho L_t}u \approx 0. \tag{52}$$

Just as in cases of double and single sided palatal snoring, a physically meaningful steady-state solution to this classical second order differential equation for displacement, u, as a function of time, t, is $u = u_{max}\cos(\omega t)$. In turn, the angular frequency $\omega = \sqrt{\frac{2c''}{\rho L_t}}$. After an initial nonzero displacement, u_{max}, the system will oscillate with a natural frequency $f = \frac{1}{2\pi}\sqrt{\frac{2c''}{\rho L_t}}$. Numerical values for the constant, c'', can be evaluated most easily using local linear regression for the function of net pressure vs. displacement, x_3. In the case of Figure 6 the natural frequency for 0.6 cm passage width between breaths (with x_3 near the 0.5 cm zero crossing) is 7 Hz with relaxed tongue muscle represented by E_t = 10 kPa, simulating deep sleep. With increased muscle tone (E_t = 60 kPa) the snoring frequency increases to 17 Hz in this example. In these cases with zero crossing points far from the posterior pharyngeal wall there would be low frequency tongue oscillations and no significant airway obstruction. However, with further narrowing of common

Channel 3, the tongue may become trapped near the zero crossing point of 0.0025 cm shown in Figure 6(c). The calculated natural frequency increases to 68 Hz, but more importantly, there is major airway obstruction in the presence of such a narrow common channel width.

In summary so far, study of the equations of Box 1 has revealed mechanisms that can produce snoring in three fundamentally different ways: double sided palatal snoring with the mouth open, single sided palatal snoring with the mouth closed, and base of tongue snoring. Under some circumstances the latter two types of snoring can lead to effort-independent, upper airway obstruction, that is, sleep apnea. The richness of possibilities is easily demonstrated in the following numerical solutions.

Numerical simulations of snoring

Validation

The mathematical model of Box 1 was implemented in Microsoft Visual Basic and validated using simple test cases having known solutions, including the idealized analytical solution for small deflection double sided palatal snoring.

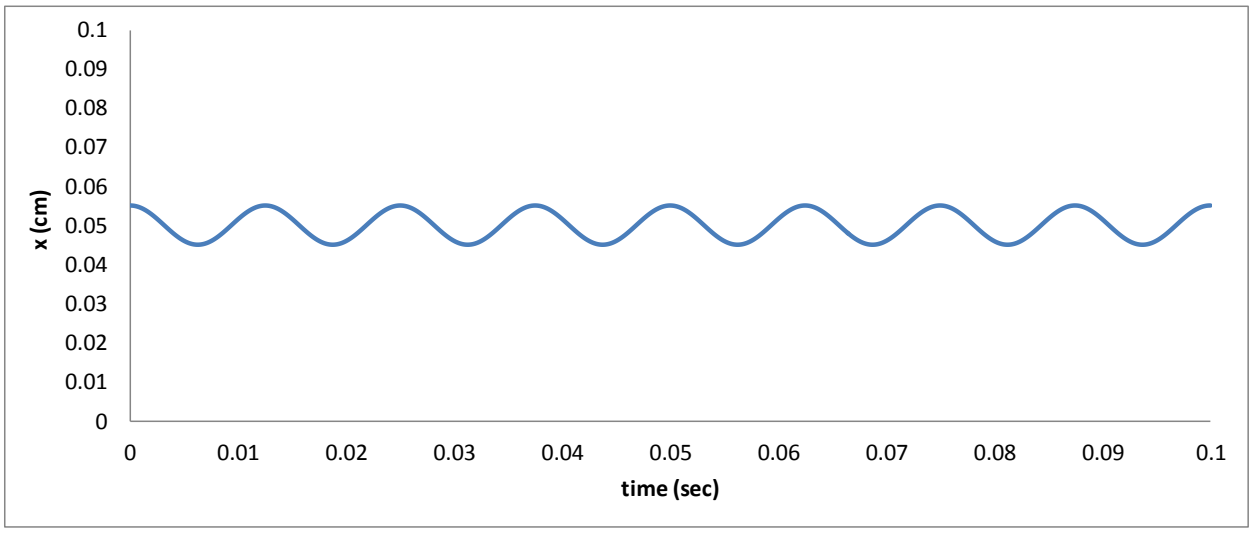

Figure 7. Numerical solutions for oscillation of soft palate for small displacement double sided palatal snoring. *Variable x_1 is plotted as a function of time. Model parameters as in Tables 1-3, except for initial palate position, shown at time zero.*

Figure 7, for example, shows the position of the soft palate, x_1, as a function of time after a small initial offset of 0.005 cm from the equilibrium position at 0.05 cm in a model of double sided palatal snoring. The numerical natural frequency of oscillation is 80.0 Hz. The corresponding analytical value from Equation (28) is 80.6 Hz.

Symmetrical double sided palatal snoring

Figure 8 shows the soft palate position as a function of time for double sided palatal snoring in the standard normal model (Tables 1 through 3). The mouth and nose are open with relatively low resistance. The start position of the palate at time zero is near the posterior wall of the pharynx, as might occur as a result of gravity with the sleeper in the supine position, or the result of residual elastic forces in tissues between breaths. In this simulation the inspiratory pressure in the lungs is a constant negative value, beginning at time zero, and the time scale is only 0.5 sec.

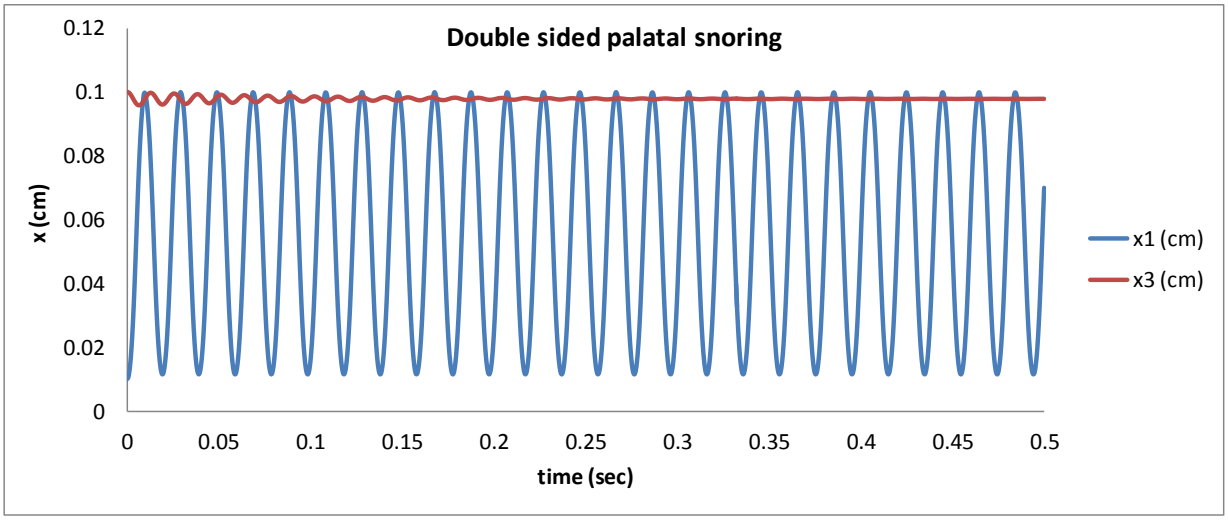

Figure 8. Numerical solutions for oscillation of soft palate for large displacement double sided palatal snoring in the standard normal model. *Variable x_1 denotes the position of the soft palate with respect to the posterior pharyngeal wall. Variable x_3 denotes position of the surface of the base of the tongue with respect to the posterior pharyngeal wall. Model parameters as in Tables 1-3.*

There is sinusoidal motion of the soft palate over most of its complete range of travel, x_{max}. The frequency of palatal oscillation is 50.5 Hz. There is no obstruction at the base of the tongue. The small base of tongue oscillations die out owing to viscoelasticity of the tongue.

Trans-palatal pressure, ΔP, for this model is shown as a function of time in Figure 9 and as a function of palatal position if Figure 10.

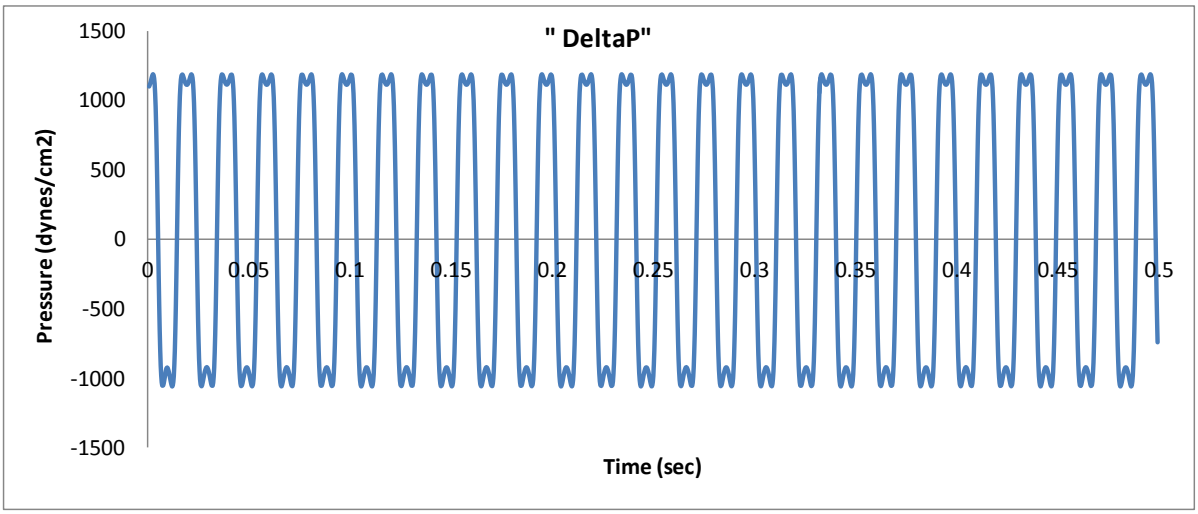

Figure 9. Trans-palatal pressure difference in the time domain in a numerical simulation of double sided palatal snoring. *Model parameters as in Tables 1-3.*

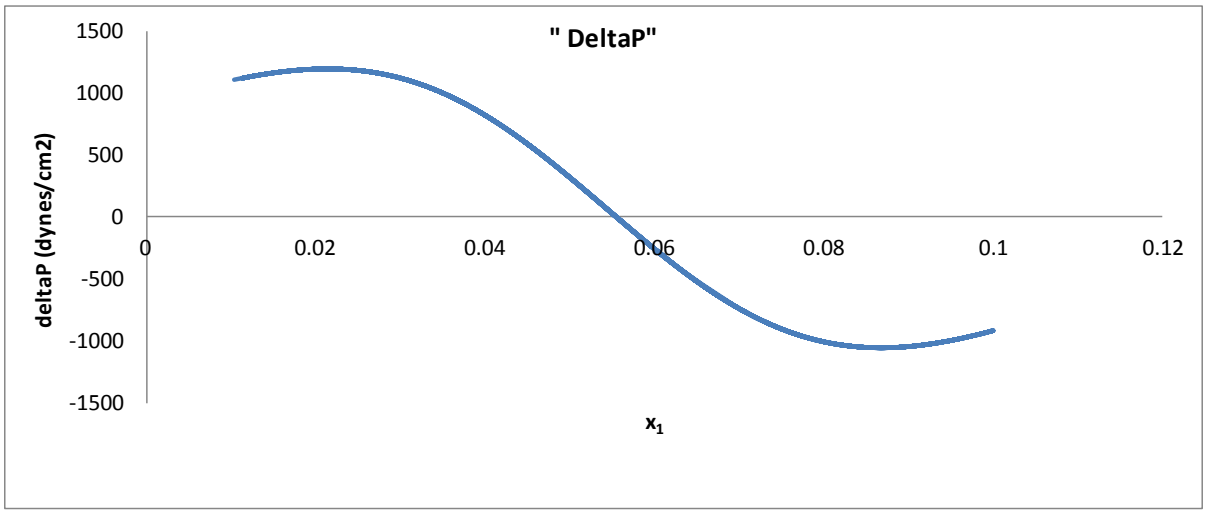

Figure 10. Trans-palatal pressure as a function of palate position in a numerical simulation of double sided palatal snoring. *Model parameters as in Tables 1-3.*

Figure 9 shows that the trans-palatal pressure difference is not sinusoidal, but rather a complex waveform in the time domain. Hence a simple analytical solution to the underlying differential equations will not do, and numerical methods are indeed needed. However, the curve in Figure 10 is similar to the simplified analytical solution in Figure 3; although the zero crossing point is slightly greater than $x_{max}/2$, here 0.055 rather than 0.050, because of unequal upstream nose and mouth resistance. (This phenomenon is described in detail in the following section on asymmetrical double sided palatal snoring.) The slope of the function at $x_1 = 0.05$ ($x_{max}/2$) is negative and corresponds to the constant, – c, in Equation (27). When the palatal position is on the nasal side of the zero crossing point, 0.055 cm in this example (see Figure 1), the trans-palatal pressure is positive, and the palate is drawn toward the zero crossing point. When the palatal position is on the oral side of the zero crossing point, the trans-palatal pressure is negative, and the soft palate is drawn back toward the zero crossing point. Cross sectional areas of the nasal side channel (A_{p1}) and the oral side channel (A_{p2}) vary accordingly as a function of palate position (Figure 11), as do the corresponding channel airflows, i_1 and i_2 (Figure 12). Total airflow and total cross sectional area remain nearly constant. In this normal case there is no significant airway obstruction. Figure 12 shows instantaneous airflow in the time domain. Average inspiratory airflow is 492 ml/sec, only slightly less than the unobstructed nominal flow of 500 ml/sec.

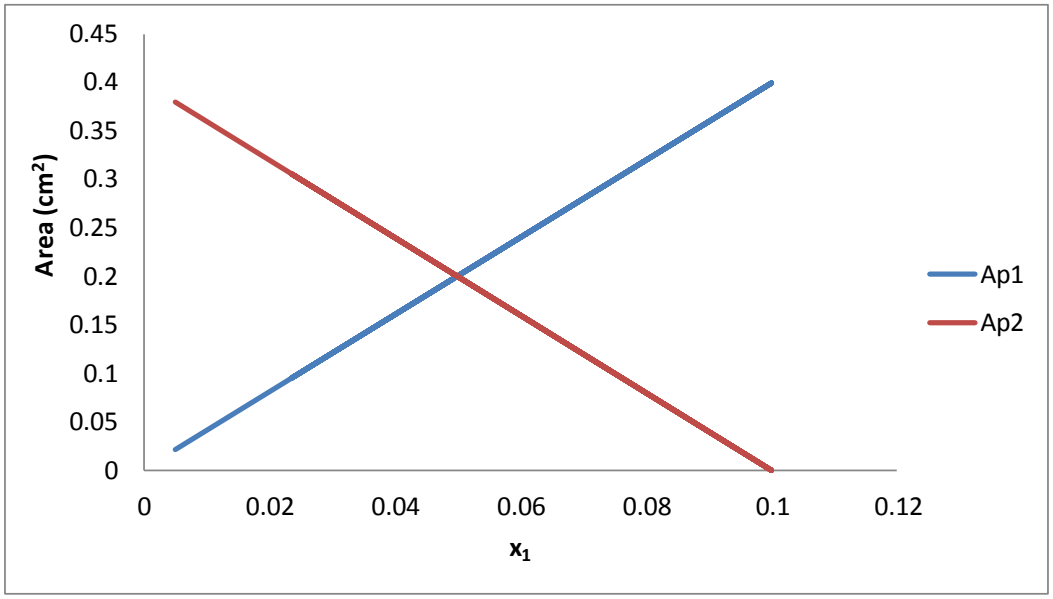

Figure 11. Cross sectional areas of spaces on the oropharyngeal (Ap1) and nasal (Ap2) sides of the soft palate in numerical simulations of double sided palatal snoring. *Model parameters as in Tables 1-3.*

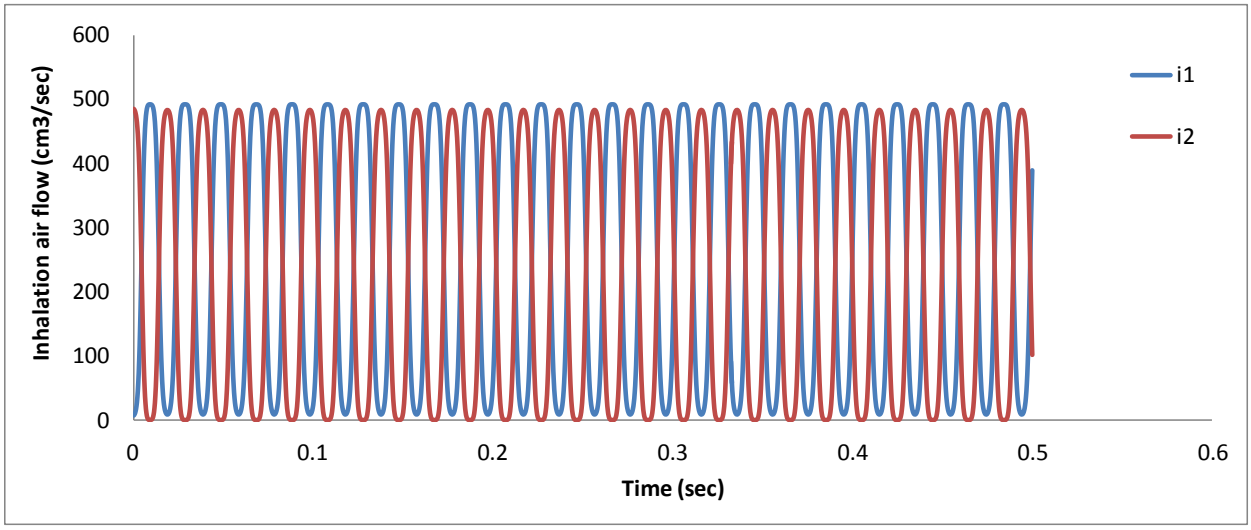

Figure 12. Air flows on the oropharyngeal (i1) and nasal (i2) sides of the soft palate in numerical simulations of double sided palatal snoring. *Model parameters as in Tables 1-3.*

With flow occurring in parallel channels on opposite sides of the soft palate the Venturi effect is greater on the side with greater airflow, not on the side with the smaller cross section (as would occur for steady flow in a single channel). If the palate is deflected either toward the nasal side or the temporal side, the net Venturi forces draw it back toward mid-position. In this normal setting the soft palate is built to fluctuate. It is no wonder that snoring is so common.

Asymmetrical double sided palatal snoring

If the mouth becomes partially, but not completely, closed, corresponding to high (50X normal) but not infinite mouth resistance, then the palatal oscillations become asymmetrical, as shown in Figure 13. Total airflow, however, remains nearly normal, 480 ml/sec, and there is little upper airway obstruction. The palatal fluctuation frequency here is about 100 Hz, which is mid-range for typical human snoring.

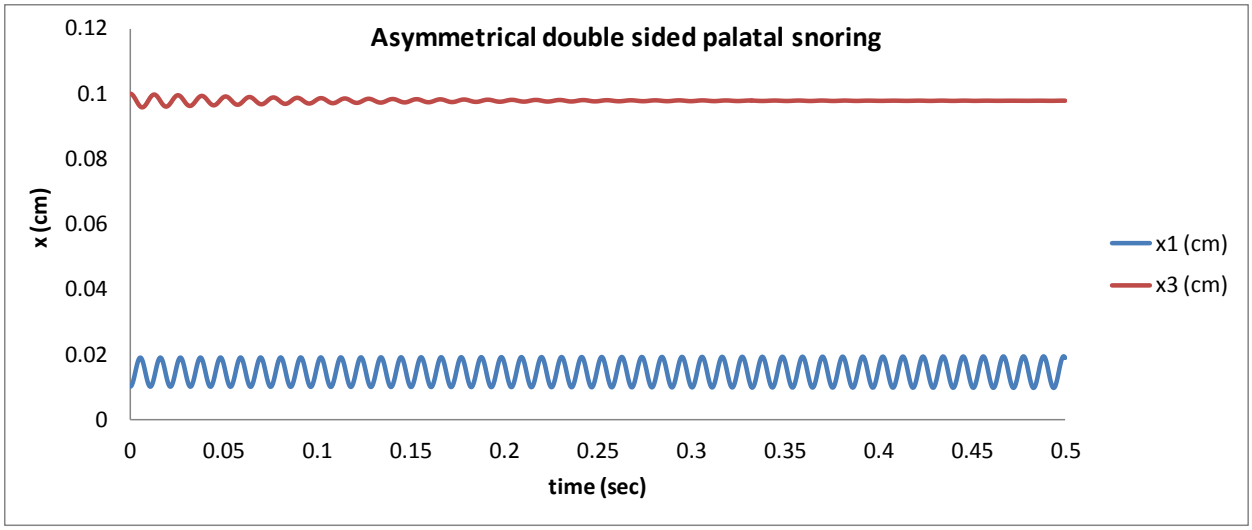

Figure 13. Numerical solutions for oscillation of soft palate for asymmetrical double sided palatal snoring in an otherwise standard normal model with 50X increased mouth resistance compared to normal, simulating a nearly, but not completely closed mouth. *Variable x_1 denotes the position of the soft palate with respect to the posterior pharyngeal wall. Variable x_3 denotes position of the surface of the base of the tongue with respect to the posterior pharyngeal wall. Other model parameters as in Tables 1-3.*

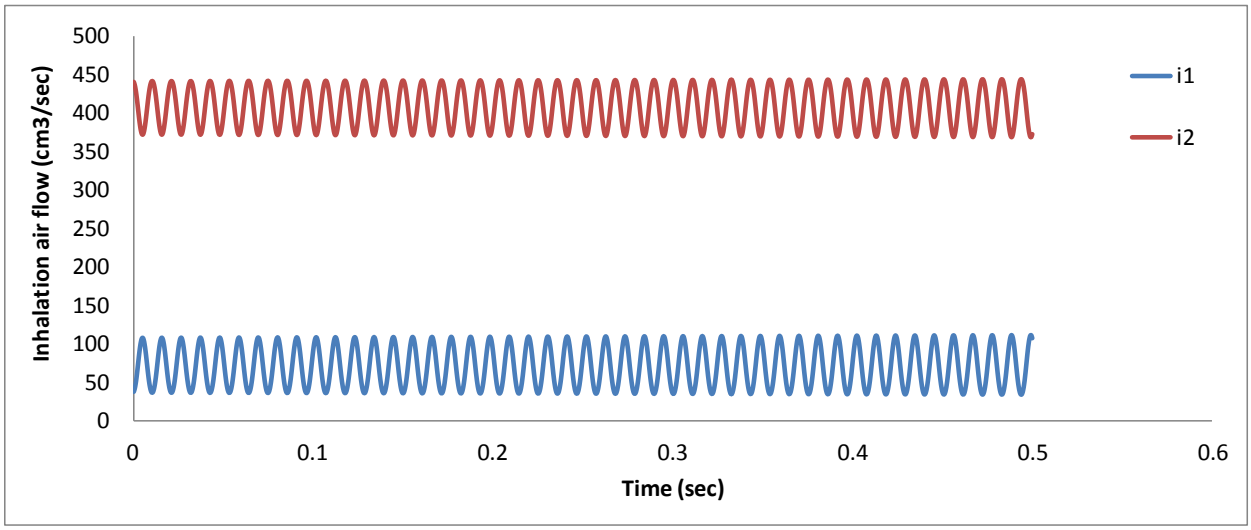

Figure 14. Numerical solutions for airflow above and below the of soft palate for asymmetrical double sided palatal snoring in an otherwise standard normal model with 50X increased mouth resistance compared to normal. *Variable i_1 denotes flow between the soft palate and the posterior pharyngeal wall. Variable i_2 denotes flow between the soft palate and base of tongue. Flow oscillations in Channels 1 and 2 are out of phase.*

In asymmetrical double-sided palatal snoring, airflow persists on both oral and nasal sides of the soft palate; however, differences in the resistance to airflow through the nose versus the mouth bias the opposing Venturi effects and the corresponding equilibrium position of the soft palate toward one side or the other, such that average trans-palatal pressure is zero (Figure 14). In this example the nasal channel (x_1) is narrowed compared to the symmetrical case, and the palate is nearer the posterior pharyngeal wall. The nasal side flow is about $1/5^{th}$ the oral side flow. However, the cross sectional area on the nasal side is also about $1/5^{th}$ that on the oral side. Hence the flow velocities on each side of the palate, and in turn the Venturi pressures, are about the same. As shown in Figure 13, the stable average position of the palate at x_1 is clearly less than $x_{max}/2$ in this example.

Frequency vs. total palatal channel width, $x_{max} = x_1 + x_2$

Changes in the total palatal channel width, x_{max}, influence the frequency of double sided palatal snoring. As shown in Figure 15(a), when the total palatal channel width is doubled, with the same relative starting position near the posterior pharyngeal wall and other parameters remaining the same, the amplitude of oscillation increases by a factor of 2 and the frequency of oscillation decreases substantially from 50 to 20 Hz. With minimal airway obstruction in the palatal region, normal snoring can still happen as a natural result of the anatomy of the airway and the Venturi effect. Even quiet sleepers may still experience palatal fluctuations at frequencies below threshold of human hearing (20 Hz).

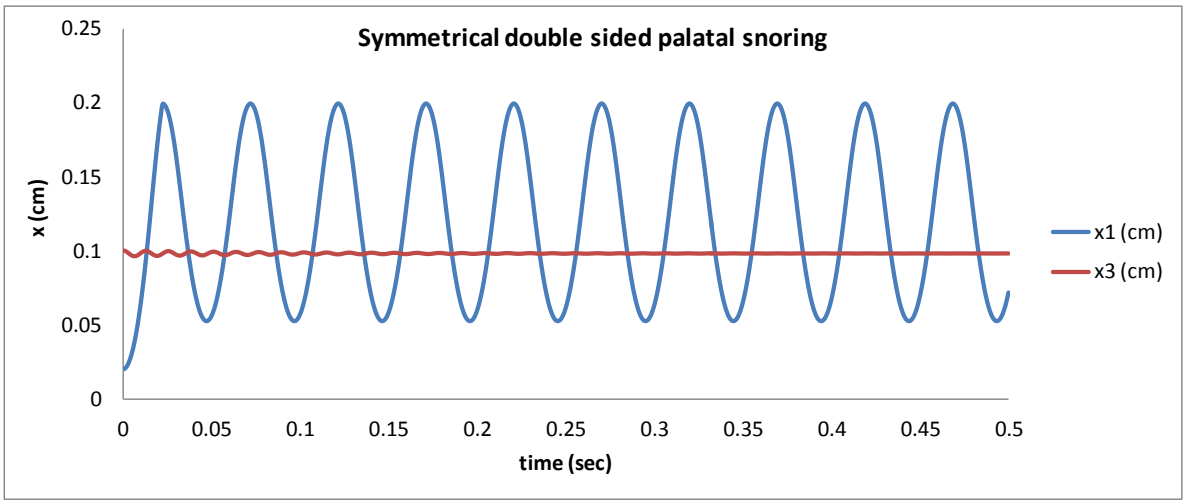

(a)

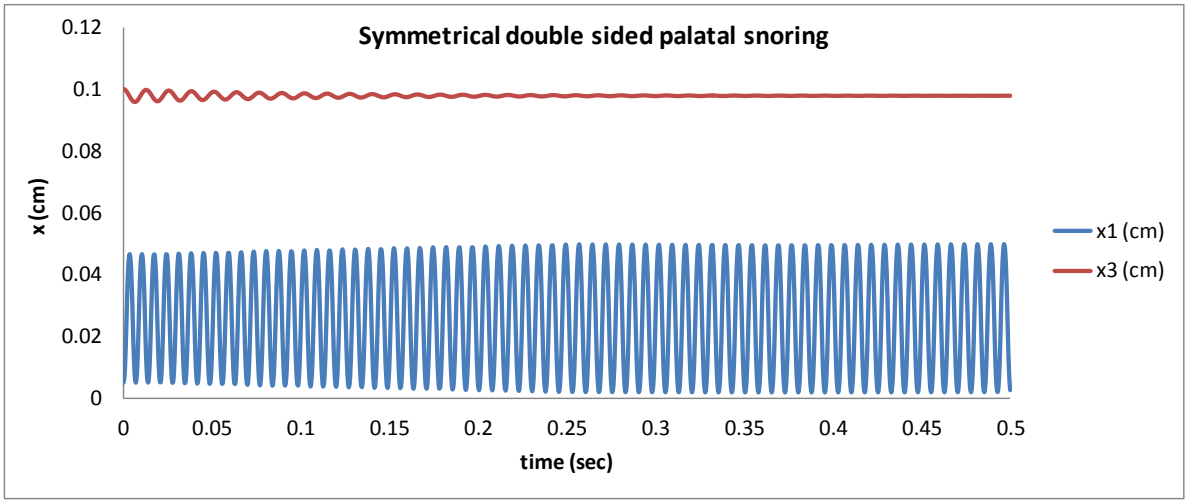

(b)

Figure 15. Numerical solutions for oscillation of soft palate and tongue for symmetrical double sided palatal snoring *in an otherwise standard normal model with (a) 2X increased clearance, x_{max}, and (b) 0.5X decreased clearance, x_{max}, between the palate and the walls of the pharynx and tongue. Variable x_1 denotes the position of the soft palate with respect to the posterior pharyngeal wall. Variable x_3 denotes position of the surface of the base of the tongue with respect to the posterior pharyngeal wall. Other model parameters as in Tables 1-3.*

Obversely, when the total palatal channel width is halved, as shown in Figure 15(b), the total travel distance decreases accordingly and the frequency of oscillation increases from 50 to 136 Hz. In general, with $f \approx \frac{1}{2\pi}\sqrt{\frac{4\rho_{air} i_{tot}^2}{s^2 x_{max}^3 \rho h}}$ (Equation (28)) the frequency is expected to be inversely related to the 3/2 power of x_{max}.

Frequency vs. common channel width

Figure 16 shows snoring frequency as a function of channel width in a scenario in which all three channels have equal slit width, which is progressively diminished. This scenario would happen, approximately, if the base of the tongue moved posteriorly. The snoring frequency spans the range of 5 to 160 Hz reported for human sleepers [7, 8, 27] and increases as the passages for airflow become progressively more narrow.

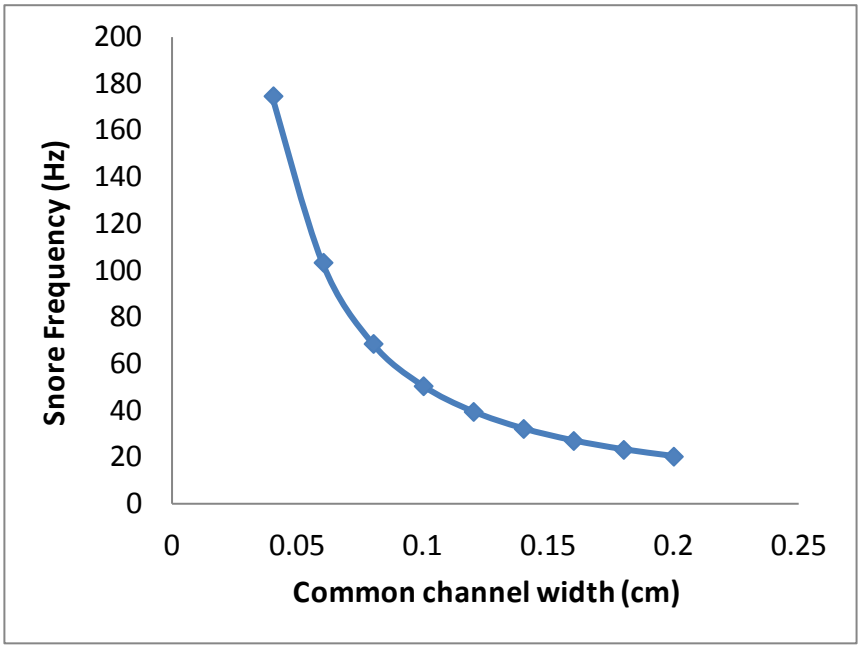

Figure 16. Snoring frequency as a function of general channel width (equal values for Channels 1, 2, and 3).

Frequency vs. lung pressure

Normal double sided snoring frequency during inspiration also depends on the magnitude of negative pressure in lungs (Figure 17). The greater the inspiratory effort, the steeper is the potential energy well for double sided palatal snoring. . With $f \approx \frac{1}{2\pi}\sqrt{\frac{4\rho_{air} i_{tot}^2}{s^2 x_{max}^3 \rho h}}$ and in this example $i \approx \frac{0 - P_{lung}}{R_{aw}}$ the frequency is expected to be directly proportional to $- P_{lung}$, as is confirmed in the numerical simulations of Figure 17.

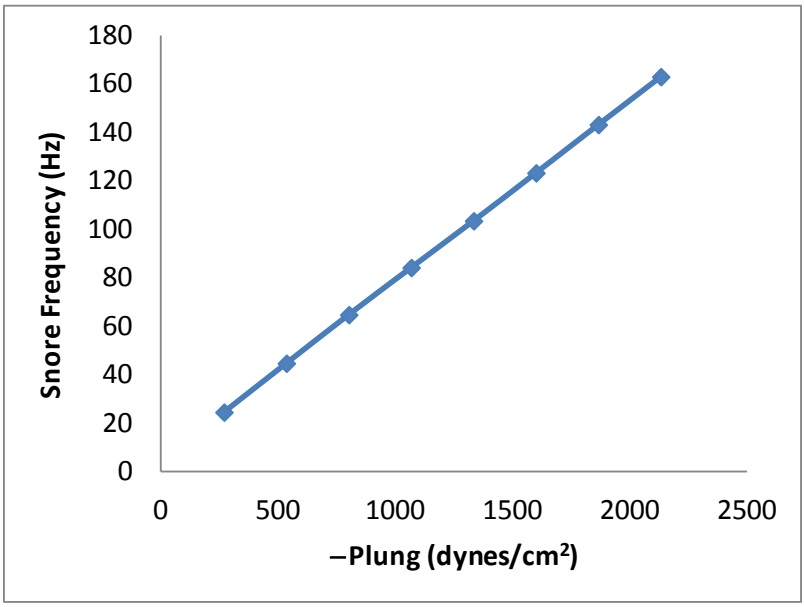

Figure 17. Palatal snoring frequency as a function of negative pressure within the lungs during inspiration in otherwise standard models.

The tradeoffs in Figures 16 and 17 can be rationalized and understood by recognizing that the spatial mean air velocity over both sides of the palate is $\bar{v} = i_{tot}/(sx_{max})$. Hence the expected natural frequency of double sided palatal snoring from Equation (28) is

$$f \approx \frac{1}{2\pi}\sqrt{\frac{4\rho_{air} i_{tot}^2}{s^2 x_{max}^3 \rho h}} \approx \frac{\bar{v}}{\pi}\sqrt{\frac{\rho_{air}}{\rho h x_{max}}}. \qquad (53)$$

Palatal snoring frequency in general is directly proportional to air flow velocity and inversely proportional to the square root of a size factor, $hx_{max} < (x_{max})^2$, where h denotes soft palate

thickness. For narrow gaps associated with snoring, one would expect $x_{max} - h$ to approach zero, or $x_{max} \approx h$. So, roughly speaking, we have

$$f \approx \frac{\bar{v}}{\pi x_{max}} \sqrt{\frac{\rho_{air}}{\rho}} . \qquad (54a)$$

Thus snoring frequency depends most importantly on the airflow velocity and the narrowness of the aggregate slit widths on both sides of the soft palate.

Further, substituting $\bar{v} = \frac{i_{tot}}{A_{tot}}$, one can re-write Equation (54a) as

$$f \approx \frac{i_{tot}}{\pi A_{tot} x_{max}} \sqrt{\frac{\rho_{air}}{\rho}} , \qquad (54b)$$

where $A_{tot} = A_{p1} + A_{p2}$ is the total airway cross section in the narrows region for double sided palatal snoring. Since i_{tot} is a physiologic constant, based on the need of the body for oxygen and since air and tissue densities are constant, the snoring frequency is, broadly speaking, simply a highly nonlinear function of the total size of the open airway in the narrows region on either side of the soft palate. Because the lower threshold for human hearing is 20 Hz, snoring can be silenced or made inaudible in principle by increasing the aggregate size of Channels 1 and 2 through interventions such as weight loss or surgery.

Effect of added damping and viscosity on palatal snoring

Figure 18 shows palatal motion for the standard model in Figure 8 with the addition of slight viscosity associated with stretching deformation of the palatal arch. The damping modulus D per unit area (D/A = 7.5 dyne-sec/cm^4), a value that is 1% of the small Young's modulus of the soft palate, multiplied by one second. Even this small amount of damping causes palatal oscillations to vanish after about 250 msec. This simulation demonstrates how highly dependent palatal snoring is on the assumption that the palate is de-tensioned and flattened in the wedge position, so that it acts as a freely moving mass in the up-down dimension, without viscous retarding forces. It appears that the small amount of damping allows vibrations induced during an inhale/exhale cycle die out before the next cycle. The 250 msec time span corresponds to brief "light" snores. With greater relaxation of pharyngeal muscles, more de-tensioning, and less influence of the palatal arch elastic and viscous elements, snores would become more prolonged. Obversely, if one adds damping, the likes of which would occur if the mid portion of the soft palate were directly supported by the palatal arches in lighter stages of sleep, double sided palatal snoring is quickly suppressed.

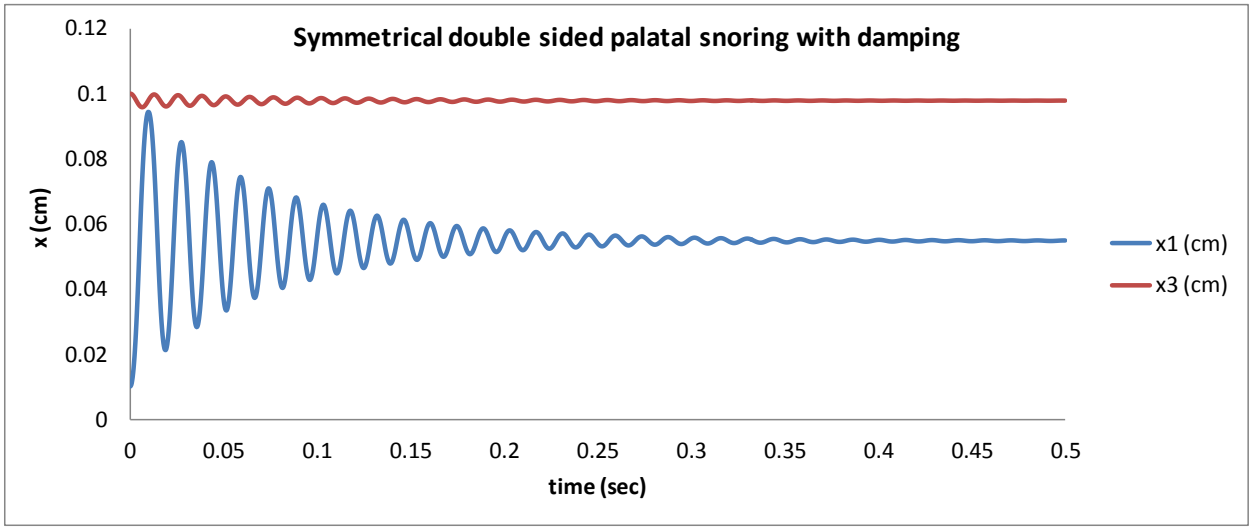

Figure 18. Numerical solutions for oscillation of the soft palate for large displacement double sided palatal snoring in the standard normal model with nonzero damping by viscoelastic attachments to the palate. *Variable x_1 denotes the position of the soft palate with respect to the posterior pharyngeal wall. Variable x_3 denotes position of the surface of the base of the tongue with respect to the posterior pharyngeal wall.*

Base of tongue snoring

Figure 19 shows an example of base of tongue snoring with the unstressed front-to-back dimension, $x_3(0)$, of common Channel 3 at a narrowed value of 3 mm, Channels 1 and 2 expanded to 9 mm, and tongue muscle stiffness at 20 kPa, representing moderate muscle tone, as might occur during light sleep. The tongue position oscillates around an equilibrium point relatively close to $x_3(0)$ and relatively far from the posterior pharyngeal wall. Total inspiratory airflow is virtually normal at 495 ml/sec, compared to the unobstructed value of 500 ml/sec. There is no sleep apnea. The frequency of tongue oscillations is about 10 Hz, well below the threshold for human hearing. This type of base of tongue "snoring" is probably not audible, but would be visible in endoscopic studies.

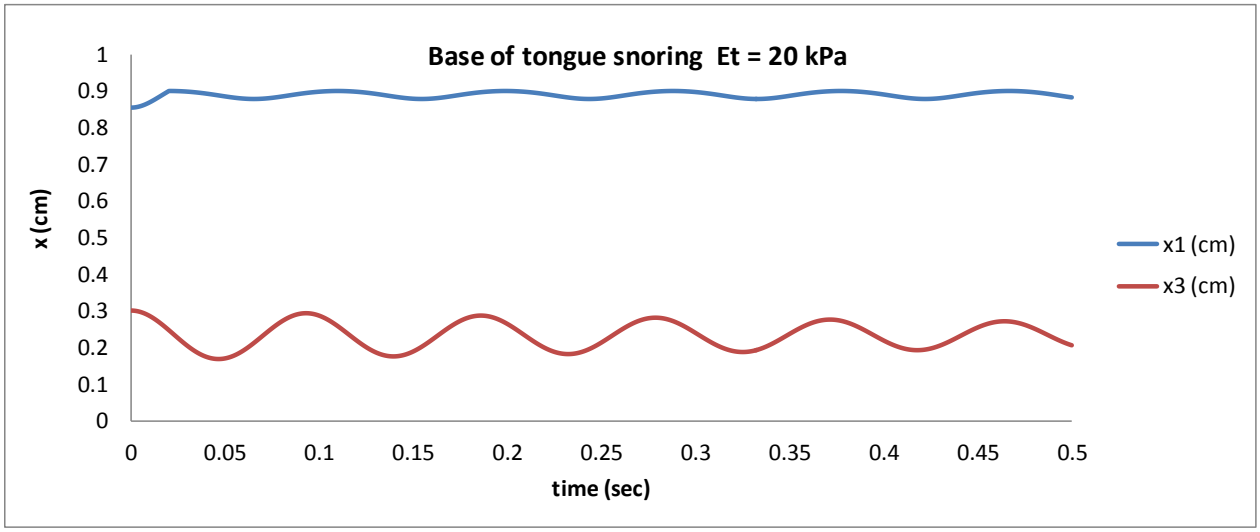

Figure 19. Numerical solutions for oscillation of base of tongue snoring in an otherwise standard normal model with tongue stiffness (E_t) reduced to about 30 percent of the normal, awake value. *Variable x_1 denotes the position of the soft palate with respect to the posterior pharyngeal wall. Variable x_3 denotes position of the surface of the base of the tongue with respect to the posterior pharyngeal wall. Model parameters as in Tables 1-3 unless otherwise noted. The time scale is expanded to one half second.*

Figure 20 shows an otherwise similar example, but with common Channel 3 further narrowed at time zero to 1.5 mm, half its previous value in Figure 19.. Now the system has found the near equilibrium point close to the posterior pharyngeal wall. Total airflow averages close to 25 ml/sec or 1/20th normal. The frequency of the small amplitude tongue oscillations after 0.025 sec is about 120 Hz, which is mid-to-upper range for common sleep sounds. The amplitude of these small tongue oscillations gradually diminishes owing to the viscoelastic properties of the tongue. Accordingly, vibrations induced during an inhale/exhale cycle die out before the next cycle. In this regime the tongue is actively trapped in a potential energy well much closer to the posterior pharyngeal wall, and the airway is significantly obstructed. This scenario represents a transition from non-pathological snoring to sleep apnea.

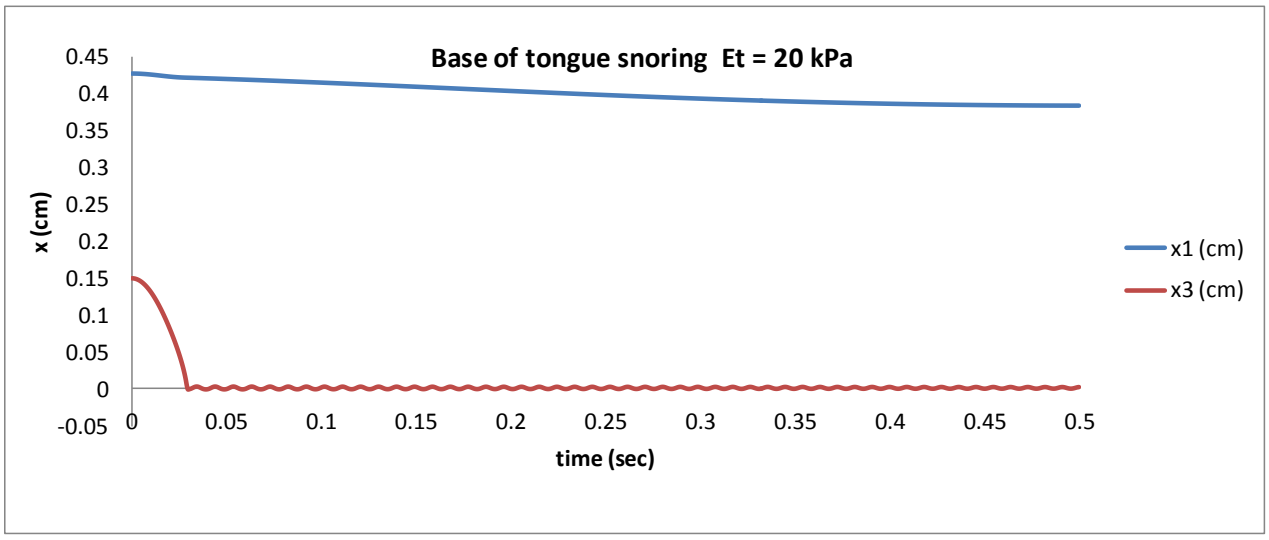

Figure 20. Numerical solutions for oscillation of base of tongue snoring in an otherwise standard normal model with tongue position twice as close (half the distance) to the posterior pharyngeal wall than in Figure 19. *Variable x_1 denotes the position of the soft palate with respect to the posterior pharyngeal wall. Variable x_3 denotes position of the surface of the base of the tongue with respect to the posterior pharyngeal wall. The monotonic fall in x represents a slow drift toward equilibrium with reduced airflow.*

Mechanisms of sleep apnea

The forgoing results suggest that snoring and sleep apnea are mechanically related and are described by the same equations. The presence of a potential energy well allows for snoring at some characteristic frequency, depending on the conditions. The location of the bottom of the potential energy well, that is, the equilibrium point, in the x-domain, determines the stable caliber of the airway locally. Owing to the complex mechanics of the upper airways, there may be one, two, or more possible potential energy wells. Which well is occupied by the system in a particular subject depends on the prevailing anatomic and physiologic parameters. Palatal snoring happens when the palate is trapped in a potential energy well in the middle of its range of travel. Sleep apnea with nasopharyngeal obstruction happens when the soft palate becomes trapped in a potential energy well close to the posterior pharyngeal wall with the mouth completely closed. Similarly, base of tongue snoring happens when the base of the tongue becomes trapped in a potential energy well relatively far from the posterior pharyngeal wall. Sleep apnea with oropharyngeal obstruction happens when the base of the tongue becomes trapped in a potential energy well close to the posterior pharyngeal wall. Accordingly, the next simulations were done to explore conditions in which motion of upper airway structures can produce virtually complete occlusion of airflow.

Single sided palatal snoring with apnea

Single sided palatal snoring is an extreme case of asymmetrical palatal snoring in which one of the parallel pathways for airflow over the palate is completely obstructed. This situation happens most commonly when the mouth is completely closed. It could also happen, in principle, during mouth breathing when the nose is completely congested.

Figure 21 illustrates palatal motion during single sided palatal snoring. In this case mouth resistance is infinite. With the mouth completely closed, airflow passes only over the nasal side of the soft palate. During inspiration the oral side of the palate is subjected to the full negative pressure in the oropharynx. This negative pressure is counterbalanced by the Venturi effect of air passing over the nasal side. The equilibrium point exists close to the wall, as shown in Figure 5, about which the palate oscillates with extremely small travel. As the nasal channel narrows and air velocity increases and the Venturi effect increases until the narrowness of the resulting gap between the palate and the posterior pharyngeal wall begins to limit total airflow. Further narrowing results in less Venturi effect with net opening pressure. The resulting equilibrium point in this scenario creates a steep potential energy well and high frequency, low amplitude oscillations.

In this scenario, illustrated by the numerical example in Figure 21, the palatal-pharyngeal gap is almost completely closed. Airway resistance is very high relative to physiological airway resistance, R_{aw}, and total airflow is close to zero (near 1.8 ml/sec vs. 500 ml/sec normally). There is effective sleep apnea. The frequency of snoring is much higher than that of double sided palatal snoring, 489 Hz in this example. It is likely to be heard as a higher pitched squeak. (Some readers may able to easily produce this sound by inhaling with the mouth tightly closed in the way some children imitate the squeal of a pig.)

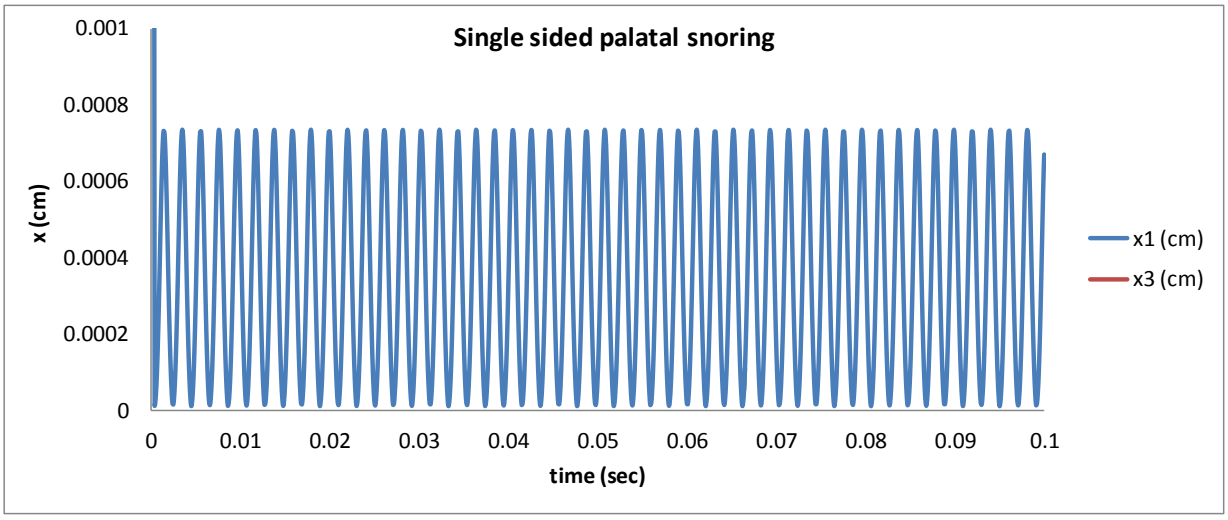

Figure 21. Single sided palatal snoring with sleep apnea. *Note absolute values on the vertical axis. The airway is essentially completely occluded. In this plot variable x3 is off scale. Note the absolute values on the vertical axis, indicating nearly complete airway occlusion when the mouth is closed.*

Base of tongue sleep apnea

Descent into sleep apnea can occur as the tongue muscle relaxes over the physiologic range of stiffness from 60 to 10 kPa or less. This sequence is shown in Figures 22(a) through 22(c), in which tongue stiffness is reduced from 60 to 20 to 10 kPa. Here the unstressed position of the tongue is at 0.3 cm from the posterior pharyngeal wall in all cases. With reduced tongue stiffness the time-averaged position of the tongue sags into the common Channel 3 as a result of negative Venturi and pulmonary pressures during inspiration. The gap, denoted by x_3 , is reduced. With a fully relaxed tongue muscle at 10 kPa there is reduced counterforce to oppose the increasing Venturi pressures. The common channel enters a new equilibrium state, predicted analytically by Equation (50), which is very close to the posterior pharyngeal wall, essentially closing the airway. As common Channel 3 closes, there is no alternative pathway. Airflow is greatly reduced (Figure 22(d)).

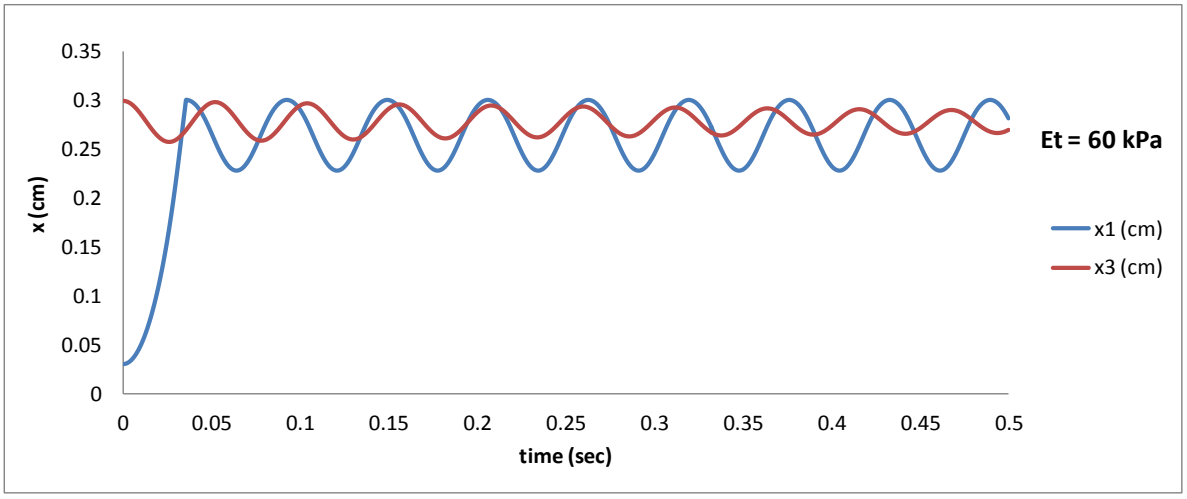

(a)

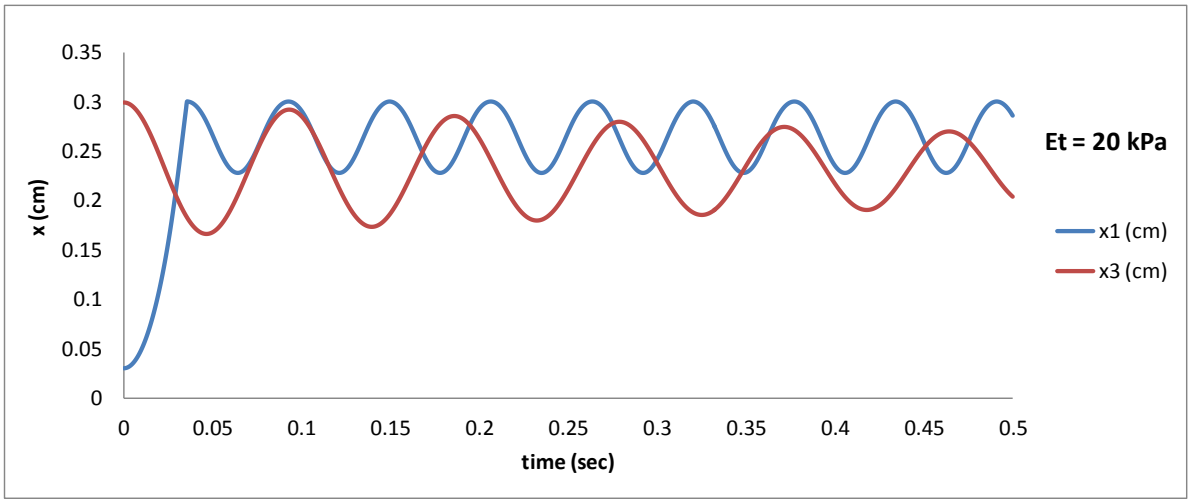

(b)

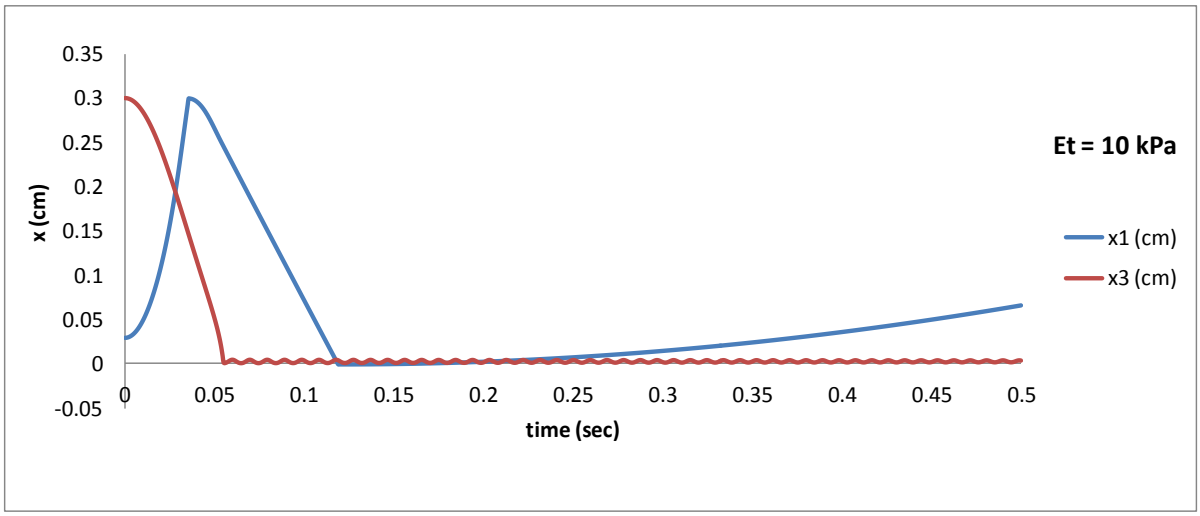

(c)

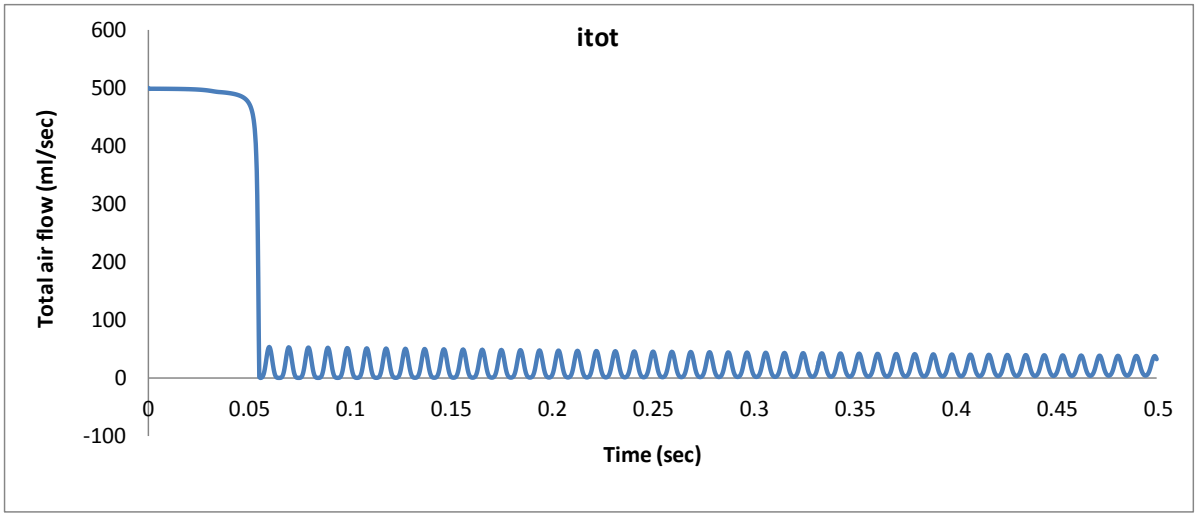

(d)

Figure 22. Decent into sleep apnea *with increasing degrees of tongue muscle relaxation simulated by progressive reduction of Young's modulus of elasticity, E_t, of the tongue (reduced stiffness) in otherwise standard models. . In (c) the monotonic rise in x_1 represents a slow drift toward equilibrium. Panel (d) shows total airflow for tongue stiffness of 10 kPa*

When further relaxation of muscles also results in more posterior positioning of the jaw, with a further reduction in $x_3(0)$, the near point equilibrium can move even closer to the posterior pharyngeal wall. In the simulation of Figure 23 the initial gap $x_3(0)$ is reduced to 1 mm with the tongue elastic modulus at 10 kPa, representing relaxed muscle tone. A similar apnea-like event occurs. Time averaged inspiratory airflow is reduced from 500 ml/sec to 1 ml/sec, representing virtually complete airway obstruction.

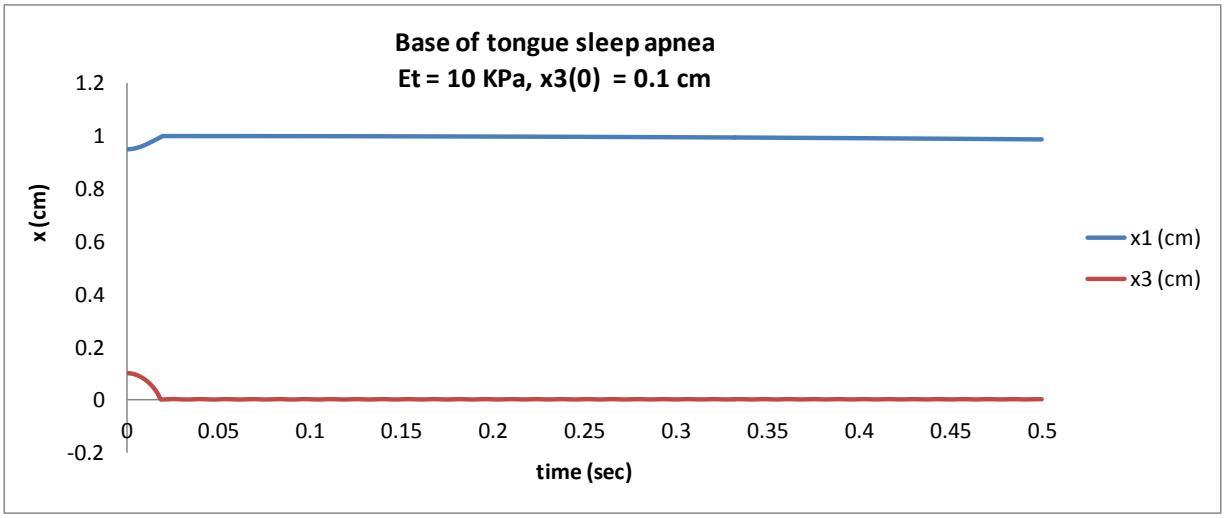

Figure 23. Palate (x1) and tongue (x3) position in models of sleep apnea created with more posterior than normal initial tongue position and reduced muscle tone.

In Figure 24 an even more extreme case is illustrated, in which complete relaxation of the tongue is modeled as a stiffness of only 5 kPa, in conjunction with a 1 mm unstressed anterior-posterior opening of the oropharynx, $x_3(0)$. In this case the equilibrium position for the base of the tongue is flush against the posterior pharyngeal wall, and inspiratory airflow is identically equal to zero. The stable equilibrium point is "behind" the posterior pharyngeal wall.

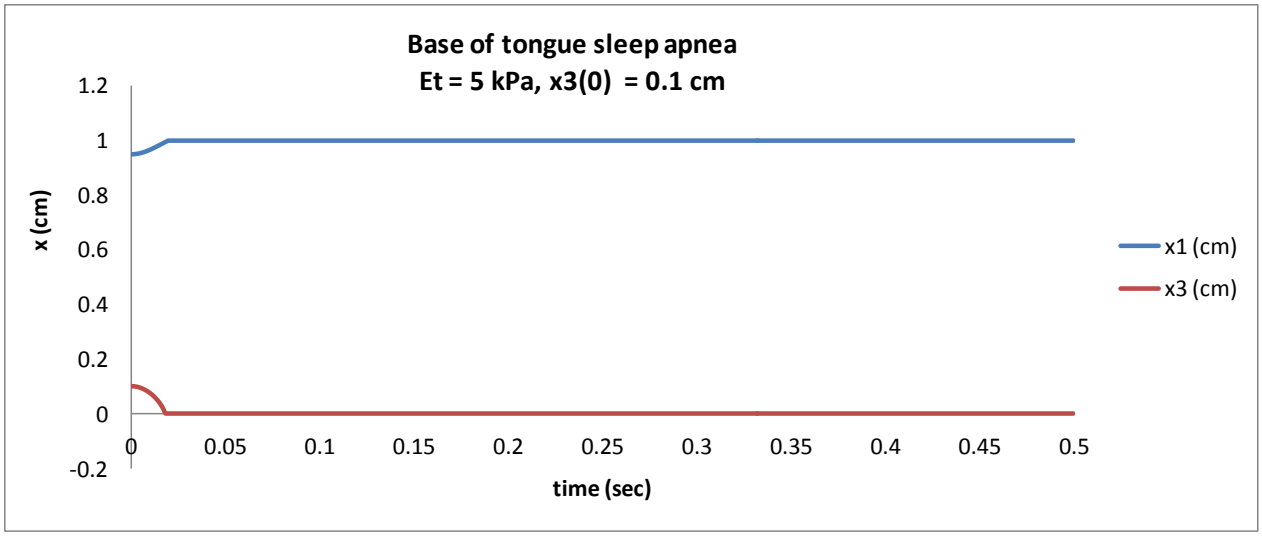

Figure 24. Palate (x1) and tongue (x3) position in models of sleep apnea with narrow unstressed oropharyngeal opening and low muscle tone. *Inspiratory airflow drops to zero.*

Discussion

Major findings

The present study has revealed new insights about the biomechanics of the most common type of snoring (mouth open, double sided palatal snoring). In particular, a proper explanation of palatal flutter must include parallel nasal and oral channels, separated by the hard and soft palates and the counterbalanced Venturi pressures on the soft palate as a function of its position. These pressures create slightly damped pendulum-like dynamics leading to palatal flutter. The free edge of the soft palate must act essentially as an unsupported simple mass with minimal viscoelastic damping. Otherwise snoring sounds would die out within a small fraction of the duration of inspiration. Palatal snoring can be symmetrical or asymmetrical. Asymmetrical palatal snoring can occur with mouth partially closed or with the nose partially congested.

Oscillations of the base of the tongue can also occur with slightly damped pendulum-like motion, either about an equilibrium point near the unstressed position of the tongue or about an equilibrium point near the posterior pharyngeal wall. Previously, Gavriely and Jensen [27] showed in a general way how base of tongue snoring could occur. They characterized forces and pressures on a narrowed segment of the upper airway that can create a potential energy well and stable oscillations under certain conditions. The present study extends this work with specific numerical calculations of waveforms and frequencies for base of tongue oscillations, which are characteristically much lower in frequency than is palatal flutter, and at times below the threshold for human hearing (20 Hz) in the frequency domain.

In addition to elucidating why common types of snoring occur, the present analysis explains why under particular conditions there can be mechanically stable, effort-independent closure of the airway in patients suffering sleep apnea. That is, it explains the physics of why sleep apnea happens and how sleep apnea and snoring are governed by the same equations. Sleep apnea can occur during nose breathing with the mouth closed, when the soft palate is pulled tightly against the posterior pharyngeal wall. The grater the inspiratory effort and negative tracheal pressure, the closer is the equilibrium of palatal position to the posterior pharyngeal wall, and the tighter the closure. In addition, sleep apnea can occur when equilibrium point for base of tongue oscillations lies very close to the posterior pharyngeal wall or even behind it. In this case the lowest potential energy state for the tongue is extremely close to, or flush against, the posterior pharyngeal wall, creating a complete obstruction of the upper airway. Increased inspiratory effort merely deepens the potential energy well and cannot reverse the apnea.

For many years various authors have speculated that the Venturi effect is related to snoring and sleep apnea. However, previous investigations have not shown in a quantitative way whether the Venturi effect generates sufficient force to move the soft palate or tongue, why under most conditions these structures oscillate rhythmically rather than simply collapsing to a stable state, and why under slightly different conditions the airway can become completely occluded and sleep apnea occurs.

The present work demonstrates how the physics of flow through parallel and series resistances, coupled with the Venturi effect, lead to governing equations that explain many facets of snoring and sleep apnea. Snoring happens when the soft palate assumes the wedge position between the tongue and the posterior pharyngeal wall, forming a Y-shaped Channel for inspired air. With limited front-to-back travel of the soft palate in the wedge position there are negligible reactive forces from bending or stretching of the anterior or lateral edges of the soft palate. In turn, the central part of the soft palate to moves as a tethered, but otherwise unsupported, mass in the dimension perpendicular to its surface. Palatal fluctuations can occur in either a symmetrical or an asymmetrical pattern. Extreme asymmetry with the mouth completely closed can lead at times to a form of sleep apnea.

In addition, if muscle relaxation and gravity allow the base of the tongue to approach the posterior oropharyngeal wall too closely, a different mechanism of snoring can occur owing to the balance between Venturi pressures that stretch the tongue and opposing elastic forces that occur because of the stretching. The balance of forces creates a potential energy well that allows the position of tongue to fluctuate, causing base of tongue snoring. When the stiffness of the tongue is reduced or the backward position of the tongue is increased because of muscle relaxation, the base of the tongue can fall into a near-wall potential energy well, forcing the tongue flush against the posterior pharyngeal wall and causing sleep apnea.

Comparison of theoretical predictions with observations

The biomechanical ideas presented in this paper explain a wide variety of experimental and clinical observations about snoring and sleep apnea.

(1) action of the palate as a simple mass

A critical feature of the present model that allows for palatal snoring is the treatment of the soft palate as a simple mass that is not constrained by its attachments to pharyngeal muscles during snoring. This idea is consistent with the observation by Trudo et al. [19] of reduced lateral diameter of pharynx during sleep. Such shrinking of lateral diameter is especially prominent in patients with sleep disordered breathing [20]. Elimination of lateral support essentially de-tensions the suspensory tissues of the soft palate during sleep, allowing the soft palate to act as an unsupported flat mass that moves in response to pressure differences between the nasopharynx and oropharynx [14].

(2) collapse sites

The present model predicts stable airway obstruction, either at the level of the soft palate or at the level of the base of the tongue, under certain conditions. These choke points have been confirmed observationally. Shepard and Thawley [4] found during non-REM sleep that 10 of 18 patients had collapse confined to the velopharyngeal or retropalatal segment of the upper airway (single sided palatal snoring with sleep apnea), and the remaining patients demonstrated collapse of the retroglossal segment of the oropharynx (base of tongue snoring with sleep apnea). Early-on Remmers and coworkers in 1978 demonstrated upper airway collapse during sleep at the level of oropharynx in patients with obstructive sleep apnea [2].

(3) snoring frequencies

In experiments on anesthetized dogs as models, Gavriely and Jensen (1993) found a mean frequency of snoring sounds near 70 Hz with a range of 30 to 100 Hz. In vivo the waveforms were non-sinusoidal with asymmetry and small higher frequency spikes (their Fig 8). However the large fundamental frequency was similar to that simulated in the present study. The anesthetized dog model of Beck [7] is similar to base of tongue snoring (with ventral human tongue-like mass created by an inflated sublingual balloon (Beck Fig. 1). This model had fundamental snore frequencies of 65-135 Hz. Beck [7] also recorded sleeping human heavy snorers and found sinusoidal frequencies ranging from 60 to 300 Hz, some with superimposed higher frequency components. Liistro and coworkers [8] found a lower time domain frequency of 25 Hz for mouth snoring, compared to 75 Hz for nose snoring. (Interestingly, the pendulum analogy presented here, was not lost on Listro, et al. 1991 who observed using cineradiography that "mouth snoring resulted in ample undulations of the whole soft palate, which was seen oscillating like a pendulum in the pharyngeal cavity"). These observed snoring frequencies are very similar to those predicted by the present biomechanical analysis and numerical model.

(4) multiple modes of snoring

The original observations of Quinn [17] of using sleep nasendoscopy, revealed at least two modes of snoring: palatal snoring, and base of tongue snoring. Independently, Liistro and coworkers [8] demonstrated two types of forced snoring in conscious subjects: mouth snoring (mouth open, nose occluded) at 32 Hz and nasal snoring (mouth closed) at 104 Hz. These experimental observations are consistent with the current theoretical treatment showing several possible snoring mechanisms with characteristically different frequencies. Perhaps Liistro's mouth and nose snoring correspond to double sided palatal snoring and single sided palatal snoring, respectively, as described in the present study.

Huang [9] using sleep nasendoscopy in sedated patients observed at least two types of soft palate vibration. In the first type with the mouth closed the "trailing edge of the soft palate [is] sucked into the nasopharyngeal space and briefly obstructing the airway before dropping back down on to the tongue below". This observation corresponds to single sided palatal snoring. In the second type observed with the mouth open, air is drawn over both the upper and lower surfaces of the soft palate, which flaps up and down. This is double sided palatal snoring. Huang et al. also observed in a smaller proportion of people, snoring associated with collapse of the pharyngeal airway below the level of the soft palate near the tongue base. This is base of tongue snoring. Hence there is observational confirmation of the modes of vibration that are predicted solely from theory in the present study. The predicted effects of increased nasal resistance on snoring have also been demonstrated in patients [33].

Conclusions

The simple one-dimensional model described herein seems to capture the essential mechanisms underlying the acoustics of snoring. It provides quantitative expressions that incorporate the physics of air flow through tubes, including the Venturi effect, the dynamics of tissue motion, and essential physiological parameters. Without introducing undue complexity, the present analysis provides physically reasonable explanations for the influence of anatomic and physiologic variables upon snoring sound frequencies. Further, the present combined one-dimensional models of soft palate and tongue dynamics explain many known phenomena of sleep apnea and snoring, including

- why snoring is so common (pendulum mechanisms and free movement of the soft palate)
- why snoring can happen with mouth closed as well as open (multiple mechanisms, including single sided vs. double sided palatal snoring and base of tongue snoring)
- why many sleepers are quiet (tongue out of wedge position, palatal or base of tongue frequency < 20 Hz)
- why sleep sounds span a wide range of frequencies between 20 and 500 Hz (multiple mechanisms and frequency dependence on total airflow, lung pressure, and variable narrows width)

- why trivial motions and changes in position can induce or eliminate snoring temporarily (re-positioning of palate over its range of travel between breaths, strong nonlinear dependence on anatomic variables)
- why sleep apnea becomes effort independent (stable equilibrium points close to the posterior pharyngeal wall)
- why sleep apnea happens with decreased muscle tone (reduced tongue spring constant and shift of equilibrium point to a position close to the posterior pharyngeal wall)
- why loud snoring can have an unpleasant, grating quality (distortion and clipping or squaring of sinusoidal waveforms as palate hits hard stops at opposite ends of its travel)
- why common palatal snoring itself is not life threatening (tradeoff between nasal and oral narrows opening widths with fluctuations in palate position)
- why palatal snoring is relatively un-damped motion and persistent throughout the duration of inspiratory airflow (pendulum like mechanism and de-tensioning of the soft palate)
- why palate travel seems slight on snoring videos (narrow channels needed to induce significant Venturi pressures)
- why common snoring can continue breath after breath (shift of palate position under gravity or residual elastic forces away from the stable equilibrium point)
- why snoring is worse with sleeper in supine position and deeper stages of sleep (shift into wedge position under gravity and tongue muscle relaxation)
- why the palate does not get stuck or migrate to an extreme position leaving one narrows channel wide open (Venturi forces operating on parallel resistive conduits draw palate toward the side of greatest airflow, creating a potential energy well)
- why weight loss or surgical removal of excess tissue can greatly reduce, but not always eliminate, snoring (nonlinear dependence of snoring frequency on dimensions of air passages and shift of frequencies toward lower, sub-audible ranges)

Applications of these insights to the treatment of snoring and sleep apnea await further research.

Author Contributions

Dr. Babbs is the sole author and is responsible for all aspects of the reported research.

Appendix 1: generalized Poiseuille law for flattened tubes with a racetrack shaped cross section

Air flow in a tube can be modeled as movement of concentric, sleeve-like shells or laminae of fluid as shown in Fig A1.1. Consider a slug of fluid of length, L, having axial pressure difference, ΔP, across it and moving through a partially flattened tube having a racetrack shaped cross section. We need to compute volumetric flow for a racetrack shape, approximating a partially collapsed, elastic tube, as shown in Fig A1.1(a) representing the upper airway passages. A center section of length, s, is flattened. The ends are semi-circular in shape with maximal inner radius, R. In the axial dimension there is laminar flow. Thin shells of fluid at variable distance, r, from the centerline also have racetrack shapes with straight segments of length, s, and curved ends of radius, r. Length, s, is a constant for any given racetrack.

(a)

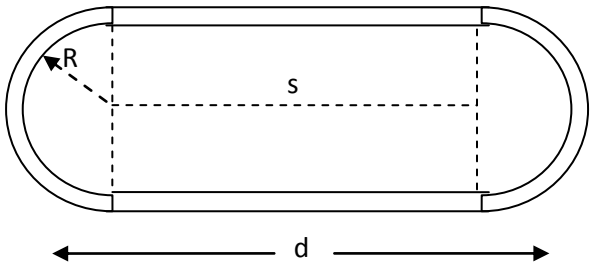

(b)

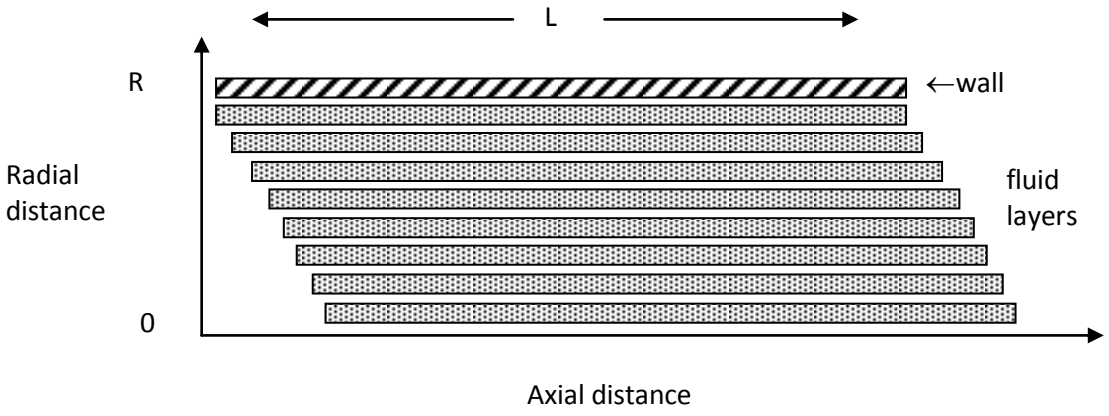

Fig A1.1. Laminar flow in the axial dimension of a partially flattened tube.

For a classical Newtonian fluid the viscous force between layers of shared surface area, A, separated by distance Δr is

$$F = \mu A \frac{\Delta u}{\Delta r}, \tag{1}$$

where μ is the viscosity, and $u(r)$ is the velocity of the shell at distance, r. For a fluid shell moving at constant velocity, u, at distance, r, Newton's second law (force = mass × acceleration) with fluid density, ρ, is

$$F = \Delta P \cdot (2\pi r + 2s) \cdot \Delta r + F_\mu = \rho \cdot (2\pi r + 2s) L \Delta r \frac{du}{dt} = 0, \tag{2}$$

where, F_μ, is the net viscous force acting on both sides of the shell at radius, r. For quasi-steady flow ($du/dt \approx 0$) we have under the steady flow assumption

$$\Delta P \cdot \Delta r + \frac{F_\mu}{2\pi(r + s/\pi)} = 0. \tag{3}$$

As shown in Box 2, the net viscous force,

$$F_\mu = 2\pi(r + s/\pi)\mu L \left(\frac{d^2u}{dr^2} + \frac{1}{r + s/\pi} \frac{du}{dr} \right) \Delta r, \tag{4}$$

so that the expanded version of Expression (3) becomes

$$0 = \Delta P \cdot \Delta r + \mu L \left(\frac{d^2u}{dr^2} + \frac{1}{r + s/\pi} \frac{du}{dr} \right) \Delta r,$$

or

$$\frac{d^2u}{dr^2} + \frac{1}{r + s/\pi} \cdot \frac{du}{dr} + \frac{\Delta P}{\mu L} = 0. \tag{5}$$

This is the fundamental differential equation for fluid velocity during steady laminar flow in the tube having a racetrack shape cross section.

Box 2: viscous forces on a racetrack shaped shell of fluid in a tube

From the definition of viscosity, $F = \mu A \frac{\Delta u}{\Delta r}$, the viscous forces acting on both the outside surface and the inside surfaces of a shell of fluid that is Δr thick at radius, r, are given by

$$
\begin{aligned}
F_\mu &= \frac{\mu L}{\Delta r}\left\{2\pi\left(r+\frac{s}{\pi}+\frac{\Delta r}{2}\right)\big(u(r+\Delta r)-u(r)\big)+2\pi\left(r+\frac{s}{\pi}-\frac{\Delta r}{2}\right)\big(u(r-\Delta r)-u(r)\big)\right\} \\
&= \frac{2\pi(r+s/\pi)\mu L}{\Delta r}\left\{\left(1+\frac{1}{2}\frac{\Delta r}{r+s/\pi}\right)\big(u(r+\Delta r)-u(r)\big)+\left(1-\frac{1}{2}\frac{\Delta r}{r+s/\pi}\right)\big(u(r-\Delta r)-u(r)\big)\right\} \\
&= \frac{2\pi(r+s/\pi)\mu L}{\Delta r}\left\{\begin{array}{l} u(r+\Delta r)+u(r-\Delta r)-2u(r) \\ +\frac{1}{2}\frac{\Delta r}{r+s/\pi}\big(u(r+\Delta r)-u(r)-u(r-\Delta r)+u(r)\big)\end{array}\right\}.
\end{aligned}
$$

Passing to the derivative,

$$F_\mu = \frac{2\pi(r+s/\pi)\mu L}{\Delta r}\left\{\left(\frac{d^2u}{dr^2}\right)(\Delta r)^2+\frac{1}{2}\frac{\Delta r}{r+s/\pi}\left(\frac{du}{dr}\right)\cdot 2\Delta r\right\}, \text{ or}$$

$$F_\mu = 2\pi(r+s/\pi)\mu L\left(\frac{d^2u}{dr^2}+\frac{1}{r+s/\pi}\frac{du}{dr}\right)\Delta r.$$

Solution of Equation (5): Consider a possible solution of the general form

$$u = a\left(k-\frac{s}{\pi}r-\frac{1}{2}r^2\right) \qquad (6a)$$

$$\frac{du}{dr} = -a\left(r+\frac{s}{\pi}\right) \qquad (6b)$$

$$\frac{d^2u}{dr^2} = -a \qquad (6c)$$

where a and k are constants to be determined.

Now using the method of undetermined coefficients to solve for constants, a and k, we have by back substitution into Equation (5), namely, $\frac{d^2u}{dr^2}+\frac{1}{r+s/\pi}\cdot\frac{du}{dr}+\frac{\Delta P}{\mu L}=0$,

$$-a+\frac{1}{r+s/\pi}\cdot -a\left(r+\frac{s}{\pi}\right)+\frac{\Delta P}{\mu L}=0\text{, or } -2a+\frac{\Delta P}{\mu L}=0\text{, giving} \tag{7a}$$

$$a=\frac{\Delta P}{2\mu L} \tag{7b}$$

Invoking the boundary condition that when r = R, u = 0 in Equation (6a) gives

$$k=R\left(\frac{s}{\pi}+\frac{1}{2}R^2\right), \tag{8}$$

and combining (6a), (7b), and (8) gives the velocity profile as a function of distance, r, namely

$$u(r)=\frac{\Delta P}{2\mu L}\left(R\left(\frac{s}{\pi}+\frac{1}{2}R^2\right)-\frac{s}{\pi}r-\frac{1}{2}r^2\right), \text{ or}$$

$$u(r)=\frac{\Delta P}{4\mu L}\left(R^2-r^2+2\frac{s}{\pi}(R-r)\right). \tag{9}$$

When r = 0, the centerline flow velocity is maximal. When r = R, the boundary condition, flow velocity is zero.

Total volumetric flow, Q, in units such as ml/sec, and in turn the resistance of the racetrack shaped tube are obtained by integration.

$$dQ=(2\pi r+2s)\cdot dr\cdot u(r)=(2\pi r+2s)\frac{\Delta P}{4\mu L}\left(R^2-r^2+2\frac{s}{\pi}(R-r)\right)dr \text{ , and } Q=\int_0^R dQ\,.$$

After multiplication and integration one obtains,

$$Q=\frac{\pi\Delta P R^4}{8\mu L}\left[1+\frac{4}{\pi}\frac{s}{R}+\frac{4}{\pi^2}\frac{s^2}{R^2}\right]. \tag{10}$$

If s = 0 Equation (10) is Poiseuille's law for laminar flow in a cylindrical tube.

The resistance to flow in the tube is the ratio of pressure difference between the ends divided by flow. Here the resistance is

$$\tilde{R} = \frac{\Delta P}{Q} = \frac{8\mu L}{\pi R^4} \cdot \frac{1}{1 + \frac{4}{\pi}\frac{s}{R} + \frac{4}{\pi^2}\frac{s^2}{R^2}} \tag{11}$$

Equation (11) describes resistance in a generalized tube with parameters R and s having a racetrack shaped cross section.

Note that if s = 0, a circular cross section, we have

$$\tilde{R} = \frac{\Delta P}{Q} = \frac{8\mu L}{\pi R^4} = \frac{8\pi\mu L}{A^2} \tag{12}$$

Now consider a relatively flattened tube with R << s. Then the resistance

$$\tilde{R} = \frac{\Delta P}{Q} = \frac{8\mu L}{\pi R^4 + 4R^3 s + \frac{4}{\pi}R^2 s^2} \tag{13a}$$

$$\tilde{R} = \frac{8\mu L}{4R^2 s^2\left(\frac{\pi R^2}{4s^2} + \frac{R}{s} + \frac{1}{\pi}\right)} \tag{13b}$$

The exact area squared is

$$A^2 = 4R^2 s^2 + \pi^2 R^4 = 4R^2 s^2\left(1 + \frac{\pi^2}{4}\frac{R^2}{s^2}\right) \tag{14}$$

For mostly flattened tubes (r/s = 0.2, for example)

$$\tilde{R} = \frac{8\pi\mu L}{A^2}. \tag{15}$$

Note that this is the same as for circular cross sections.

More exactly, substituting $A^2 = 4R^2s^2\left(1+\frac{\pi^2}{4}\frac{R^2}{s^2}\right)$ in $\widetilde{R} = \frac{8\mu L}{4R^2s^2\left(\frac{\pi R^2}{4s^2}+\frac{R}{s}+\frac{1}{\pi}\right)}$,

$$\widetilde{R} = \frac{8\mu L\left(1+\frac{\pi^2}{4}\frac{R^2}{s^2}\right)}{A^2\left(\frac{\pi R^2}{4s^2}+\frac{R}{s}+\frac{1}{\pi}\right)} \tag{16a}$$

$$\widetilde{R} = \frac{8\mu L\left(s^2+\frac{\pi^2R^2}{4}\right)}{A^2\left(\frac{\pi R^2}{4}+sR+\frac{s^2}{\pi}\right)}, \tag{16b}$$

and when s = 0 or when R << s, $\widetilde{R} = \frac{8\pi\mu L}{A^2}$.

The ratio $\theta = \frac{\widetilde{R}}{\frac{8\pi\mu L}{A^2}} = \frac{1}{\pi}\frac{s^2+\frac{\pi^2R^2}{4}}{\frac{\pi R^2}{4}+sR+\frac{s^2}{\pi}} = \frac{s^2+\frac{\pi^2R^2}{4}}{\frac{\pi^2R^2}{4}+sR\pi+s^2} = \frac{1}{1+\frac{sR\pi}{s^2+\frac{\pi^2R^2}{4}}}$, or

$$\theta = \frac{1}{1+\frac{\pi}{\frac{s}{R}+\frac{\pi^2}{4}\frac{R}{s}}}. \tag{17}$$

If s/R = 0, a circle or if R/s = 0, a slit we have θ = 1. Let c = s/R, the compression factor, or shape factor. Then

$$\theta = \frac{1}{1+\frac{\pi}{c+\frac{\pi^2}{4c}}} = \frac{1}{1+\frac{\pi c}{c^2+\pi^2/4}}. \tag{18}$$

Theta is a shape factor between 0.5 and 1.0. For typical pharyngeal shapes θ ~ 0.6, as shown in Figure A1.2

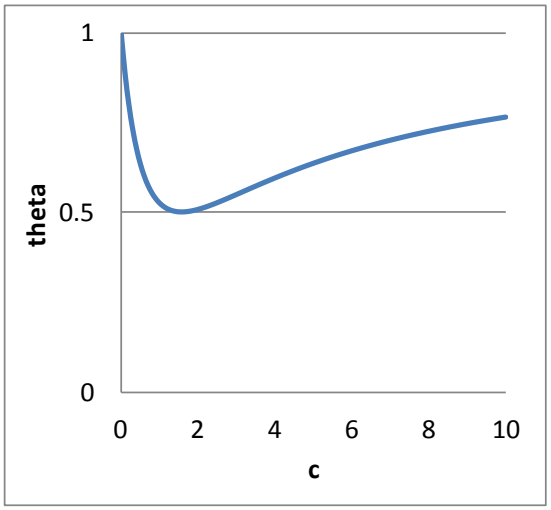

Fig A1.2. Shape factor plotted as a function of compression factor c = s/R.

Appendix 2: the Venturi effect with Ohmic resistance

Figure A2.1 shows a sketch of air, as a compressible fluid, flowing through a narrowing passageway. The larger reference cross section of the passage in section 1 (left) is denoted A_0 and the smaller narrow cross section of the passage in section 2 (right) is denoted A_n. There is continuous flow through the tube, and the total flow through the reference segment 0 equals the total flow through the narrowed segment at location, x, in quasi-steady state.

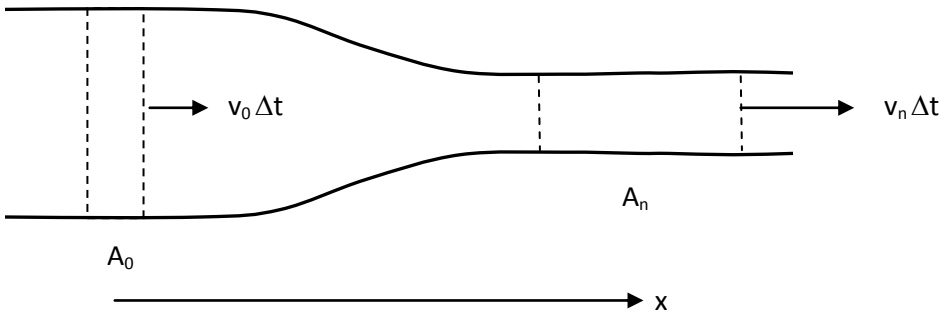

Figure A2.1. Scheme for the Venturi effect.

By conservation of energy, the total energy of the volume $V_n = A_n v_n \Delta t$ equals the total energy of volume $V_0 = A_0 v_0 \Delta t$, minus any frictional energy loss due to resistance of the tube. The total energy of each volume is the sum of its potential energy and its kinetic energy. For the compressible gas the potential energy is the product of its pressure and volume, PV. The kinetic

energy is one half mass times velocity. Hence, using U to denote energy, m to denote mass, and subscripts p and k for potential and kinetic energy, we have for potential energy

$$U_{p0} = P_0 A_0 v_0 \Delta t\,,\ U_{pn} = P_n A_n v_n \Delta t\,.$$

For kinetic energy

$$U_{k0} = \frac{1}{2} m_0 v_0^2,\ U_{kn} = \frac{1}{2} m_n v_n^2,$$

and for air density, ρ,

$$m_0 = \rho A_0 v_0 \Delta t\,,\ m_n = \rho A_n v_n \Delta t\,,$$

so that

$$U_{k0} = \frac{1}{2} \rho A_0 v_0^3 \Delta t\,,\ U_{kn} = \frac{1}{2} \rho A_n v_n^3 \Delta t\,.$$

Let the flow in the tube be denoted as i and the resistance from a reference point, 0, in the axial dimension be R(x), such that R(0) = 0

$$R(x) = \int_0^x dR\,.$$

and for air viscosity, μ, and Poiseuille type resistance for a flattened tube or for a slit-like opening described by shape factor, θ, we have $dR = \theta \frac{8\pi\mu}{A^2(x)} dx$, as shown in Appendix 1.

The energy loss in time Δt from friction due to resistance of the tube along axial path 0 to x is $i^2 R(x)\Delta t$. So that in terms of total energy, U_{tot} = potential energy plus kinetic energy

$$U_{tot}(x) = U_{tot}(0) - i^2 \Delta t \int_0^x dR\,.$$

Expanding in terms of potential and kinetic energy, with velocity, v = i/A, and volume, V = iΔt,

$$P_n A_n v_n \Delta t + \frac{1}{2} m_n v_n^2 = P_0 A_0 v_0 \Delta t + \frac{1}{2} m_0 v_0^2 - i^2 \Delta t \int_0^x dR$$

$$P_n i \Delta t + \frac{1}{2} \rho i \Delta t \cdot \frac{i^2}{A_n^2} = P_0 i \Delta t + \frac{1}{2} \rho i \Delta t \cdot \frac{i^2}{A_0^2} - i^2 \Delta t \int_0^x dR\,.$$

Now, solving for the local pressure at axial distance, x,

$$P_x = P_0 - \frac{1}{2}\rho i^2\left(\frac{1}{A_n^2} - \frac{1}{A_0^2}\right) - i\int_0^x dR$$

If the cross sectional areas are equal, we have Ohm's law. If the frictional resistance is zero we have the Venturi equation. The combined expression gives the pressure drop in the presence of nonzero airway resistance and changing cross sectional area.

Appendix 3 reactive spring constant/area for palatopharyngeal arch under tension

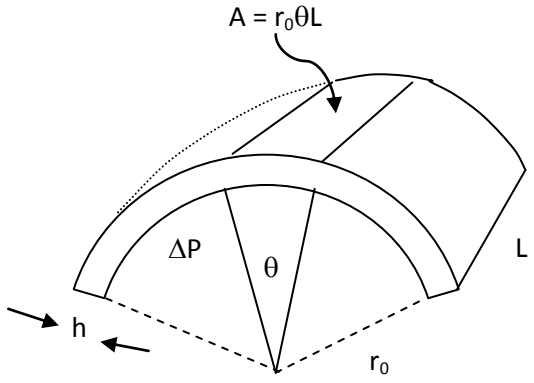

Figure A3.1. Geometric model of soft palate as an arch of constant curvature.

In Figure A3.1 the soft palate is modeled as a segment of a cylindrical arch of constant curvature, having wall thickness, h, unstressed radius, r_0, and length, L. Consider an expanding transmural pressure, ΔP, acting on an angular sector, θ, of the arch, which represents the middle portion of the soft palate that fluctuates in palatal snoring. We are interested in specifying the spring constant relating the incremental force ΔF, as a result of pressure ΔP, and the corresponding incremental change in radius, Δr, which represents the upward shift in the midline soft palate position. The effective spring constant is defined as $k = \frac{\Delta F}{\Delta r}$, and $\frac{k}{A} = \frac{\Delta P}{\Delta r}$.

From the Law of Laplace, we have the expression for circumferential wall stress, σ, in a segment of a thin walled elastic cylinder, $\sigma = \Delta P \frac{r_0}{h}$. Young's modulus, $E = \frac{\sigma}{\frac{\Delta r}{r_0}}$, relates wall stress and

strain, so $\Delta P = \sigma \frac{h}{r_0} = E \frac{\Delta r h}{r_0^2}$. Force increment $\Delta F = \Delta P \cdot A = \Delta P \cdot r_0 \theta L = E \frac{\Delta r h}{r_0^2} \cdot r_0 \theta L$. Thus the spring constant, k = ΔF/Δr, is $k = E \frac{h}{r_0} \cdot \theta L$, and the spring constant per unit area is $\frac{k}{A} = E \frac{h}{r_0^2}$.

References

1. Ayappa I, Rapoport D. The upper airway in sleep: physiology of the pharynx. *Sleep Medicine Reviews* 2003; **7**: 9-33.
2. Remmers J, deGroot W, Sauerland E, Anch A. Pathogenesis of upper airway occlusion during sleep. *j Appl Physiol: Respirat. Environ. Exercise Physiol.* 1978; **44**: 931-938.
3. Walsh R, EDMichaelson, Harkleroad L, Zighelboim A, Sackner M. Upper airway obstruction in obese patients with sleep disturbance and somnolence. *Ann Intern Med* 1972; **76**: 185-192.
4. Shepard J, Thawley S. Localization of upper airway collapse during sleep in patients with obstructive sleep apnea. *Am Rev Respir Dis* 1990; **141**: 1350-1355.
5. Strollo P, Rogers R. Obsgtructive sleep apnea. *New England J. Med* 1996; **334**: 99-104.
6. Liistro G, Stanescu D, Veriter C, Rodenstein D, Aubert-Tulkens G. Pattern of snoring in obstructive sleep apnea patients and in heavy snorers. *Sleep Medicine Reviews* 1991; **14**: 517-525.
7. Beck R, Odeh M, Oliven A, Gavriely N. The acoustic properties of snores. *Eur Respir J* 1995; **8**: 2120-2128.
8. Liistgro G, Stanescu D, Veriter C. Pattern of simulated snoring is different through mouth and nose. *J Appl Physiol* 1991; **70**: 2736-2741.
9. Huang L, Quinn S, Ellis P, Williams J. Biomechanics of snoring. *Endeavour* 1995; **19**: 96-100.
10. Reda M, Sims A, Collins M, McKee G, al e. Morphological assessment of the soft palate in habitual snoring using image analysis. *The Laryngoscope* 1999; **109**: 1655-1660.
11. Rojewski T, Schuller D, Schmidt H, Clark R, Potts R. Synchronous video recording of the pharyngeal airway and polysomnograph in patients with obstructive sleep apnea. *Laryngoscope* 1982; **92**: 246-250.
12. Polo O, Tafti M, Fraga J, Porkka K, Dejean Y, Billiard M. Why don't all heavy snorers have obstructive sleep apnea? *Am Rev Respir. Dis* 1991; **143**: 1288-1293.
13. White D. Occlusion pressure and ventilation during sleep in normal humans. *J Appl Physiol* 1986; **61**: 1279-1287.
14. Morrell M, Badar M. Effects of REM sleep on dynamic within-breath changes in upper airway patency in humans. *J Appl Physiol* 1998; **84**: 190-199.
15. Skatrud J, Dempsey J. Airway resistance and respiratory muscle function in snorers during NREM sleep. *J Appl Physiol* 1985; **59**: 328-335.
16. Stoohs R, Guilleminault C. Snoring during NREM sleep: respiratory timing, esophageal pressure and EEG arousal. *Respir Physiol* 1991; **85**: 151-167.
17. Quinn S, Daly N, Ellis P. Observation of the mechanism of snoring using sleep nasendoscopy. *Clin Otolaryngol* 1995; **20**: 360-364.

18. Mallampati S, Gatt S, Gugino L, Desai S, WSaraksa B, Freiberger D, Liu P. A clinical sign to predict difficult tracheal intubation: a prospective study. *Canadian Anesthesia Society Journal* 1985; **32**: 429-434.
19. Trudo F, Gefter W, Welch K, Gupta K, Maislin G, SChway R. State-related changes in upper airway caliber and surrounding soft-tissue structures in normal subjects. *Am J Respir Crit Care Med* 1998; **158**: 1259-1270.
20. Schwab R, Gupta K, Gefter W, Metzger L, Hoffman E, Pack A. Upper airway and soft tissue anatomy in normal subjects and patients with sleep-disordered breathing: significance of the lateral pharyngeal walls. *Am J Respir Crit Care Med* 1995; **152(5 Pt 1)**: 1673-1689.
21. Birch M, Srodon P. Biomechanical properties of the human soft palate. *Cleft Palate-Craniofacial Journal* 2009; **46**: 268-274.
22. Chen E, Novakofski J, Jenkins W, O'Brien W. Young's modulus measurements of soft tissues with application to elasticity imaging. *IEEE Transactions on Ultrasonics, Ferroelectrics, and Frequency Control* 1996; **43**: 191-194.
23. Cheng S, Gandevia S, Green M, Sinkus R, Bilston L. Viscoelastic properties of the tongue and soft palate using MR elastography. *J Biomechanics* 2011; **44**.
24. Payan Y, Bettega G, Raphael B. A biomechanical model of the human tongue and its clinical implications. *MICCAI'98* 1998; **LNCS 1496**: 688-695.
25. Brown I, Bradley T, Phillipson E, Zamel N, Hoffstein V. Pharyngeal compliance in snoring subjects with and without obstructive sleep apnea. *Am Rev Respir Dis* 1985; **132**: 211-215.
26. Huang Y, White D, Malhotra A. Use of computational modeling to predict responses to upper airway surgery in obstructive sleep apnea. *Laryngoscope* 2007; **117**: 648-653.
27. Gavriely N, Jensen O. Theory and measurements of snores. *J Appl Physiol* 1993; **74**: 2828-2837.
28. Shinohara M, Sabra K, Gennisson J, Fink M, Tanter M. Real-time visualization of muscle stiffness distribution with ultrasound shear wave imaging during muscle contraction. *Muscle & Nerve* 2010; **42**: 438-441.
29. Duck F. *Physical Properties Of Tissue: A Comprehensive Reference Book.* Academic Press: London, 1990.
30. Comley K, Fleck N. A micromechanical model for the Young's modulus of adipose tissue. *International Journal of Solids and Structures* 2010; **47**: 2982-2990.
31. Krouskop T, Wheeler T, Kallel F, Garra B, Hall T. Elastic moduli of breast and prostate tissues under compression. *Ultrasonic Imaging* 1998; **20**: 260-274.
32. Cheng S, Butler J, Gandevia S, Bilston L. Movement of the tongue during normal breathing in awake healthy humans. *J Physiol* 2880; **586 (Pt 17)**: 4283–4294.
33. Young T, Finn L, Palta M. Chronic nasal congestion at night is a risk factor for snoring in a population-based cohort study. *Arch Intern Med* 2001; **161**: 1514-1519.